

12 **Abstract:**

13 Southeast coastal region is one of the most developed and populated area in China.
14 Meanwhile, it has been a severe acid rain impacted region for many years. The chemical
15 compositions and carbon isotope composition ratio of dissolved inorganic carbon
16 ($\delta^{13}\text{C}_{\text{DIC}}$) of river waters in high flow season were investigated to evaluate the chemical
17 weathering and associated atmospheric CO_2 consumption rates. Mass balance
18 calculation indicated that the dissolved loads of major rivers in the Southeast Coastal
19 Rivers Basin (SECRB) were contributed by atmospheric (14.3%, 6.6-23.4%),
20 anthropogenic (15.7%, 0-41.1%), silicate weathering (39.5%, 17.8-74.0%) and
21 carbonate weathering inputs (30.6%, 3.9-62.0%). The silicate and carbonate chemical
22 weathering rates for these river watersheds were $14.2\text{-}35.8 \text{ t km}^{-2} \text{ a}^{-1}$ and $1.8\text{-}52.1 \text{ t km}^{-2}$
23 a^{-1} , respectively. The associated mean CO_2 consumption rate by silicate weathering
24 for the whole SECRB were $191 \times 10^3 \text{ mol km}^{-2} \text{ a}^{-1}$. The chemical and $\delta^{13}\text{C}_{\text{DIC}}$ evidences
25 indicated that sulfuric and nitric acid (mainly from acid deposition) was significantly
26 involved in chemical weathering of rocks. The calculation showed an overestimation
27 of CO_2 consumption at $0.19 \times 10^{12} \text{ g C a}^{-1}$ if sulfuric and nitric acid was ignored, which
28 accounted for about 33.6% of the total CO_2 consumption by silicate weathering in the
29 SECRB. This study quantitatively highlights that the role of acid deposition in chemical
30 weathering, suggesting that anthropogenic impact should be seriously considered in
31 estimation of chemical weathering and associated CO_2 consumption.

32

33 **1. Introduction**

34 Chemical weathering of rocks is the key process that links geochemical cycling of
35 solid earth to the atmosphere and ocean. It provides nutrients to terrestrial and marine
36 ecosystems and regulates the level of atmospheric CO₂. As a net sink of atmospheric
37 CO₂ on geologic timescales, estimation of silicate chemical weathering rates and the
38 controlling factors are important issues related to long-term global climate change (e.g.
39 Raymo and Ruddiman, 1992; Négrel et al. 1993; Berner and Caldeira, 1997; Gaillardet
40 et al., 1999; Kump et al., 2000; Amiotte-Suchet et al., 2003; Oliva et al., 2003;
41 Hartmann et al., 2009; Moon et al., 2014). As an important component in the Earth's
42 Critical Zone (U.S. Nat. Res. Council Comm., 2001), river serves as an integrator of
43 various natural and anthropogenic processes and products in a basin, and a carrier
44 transporting the weathering products from continent to ocean. Therefore, the chemical
45 compositions of river waters are widely used to evaluate chemical weathering and
46 associated CO₂ consumption rates at catchment and/or continental scale, and examine
47 their controlling factors (e.g., Edmond et al., 1995; Gislason et al., 1996; Galy and
48 France-Lanord, 1999; Huh, 2003; Millot et al., 2002, 2003; Oliva et al., 2003; West et
49 al., 2005; Moon et al., 2007; Noh et al., 2009; Shin et al., 2011; Calmels et al., 2011;
50 Li, S., et al. 2014).

51 With the intensification of human activities, human perturbations to river basins
52 have increased in frequency and magnitude (Raymond et al., 2008; Regnier et al., 2013;
53 Li and Bush, 2015). It is important to understand how such perturbations function on
54 the current weathering systems and to predict how they will affect the Critical Zone of
55 the future (Brantley and Lebedeva, 2011). In addition to CO₂, other sources of acidity

56 (such as sulfuric, nitric and organic acids) can also produce protons. These protons react
57 with carbonate and silicate minerals, thus enhance rock chemical weathering rate and
58 flux compared with only considering protons deriving from CO₂ dissolution (Calmels
59 et al., 2007; Xu and Liu, 2010). The effect of other sourced proton (especially H⁺
60 induced by SO₂ and NO_x coming from anthropogenic activities) on chemical
61 weathering is documented to be an important mechanism modifying atmospheric CO₂
62 consumption by rock weathering (Galy and France-Lanord, 1999; Semhi, et al., 2000;
63 Spence and Telmer, 2005; Xu and Liu, 2007; Perrin et al., 2008; Gandois et al., 2011).
64 Anthropogenic emissions of SO₂ was projected to provide 3 to 5 times greater H₂SO₄
65 to the continental surface than the pyrite oxidation originated H₂SO₄ (Lerman et al.,
66 2007). Therefore, increasing acid precipitation due to intense human activities
67 nowadays could make this mechanism more prominently.

68 The role of acid precipitation plays on the chemical weathering and CO₂
69 consumption has been investigated in some river catchments (Amiotte-Suchet et al.,
70 1995; Probst et al., 2000; Vries et al., 2003; Lerman et al., 2007; Xu and Liu, 2010). It
71 has been documented that silicate rocks were more easily disturbed by acid
72 precipitation during their weathering and soil leaching processes, because of their low
73 buffering capacity (Reuss et al., 1987; Amiotte-Suchet et al., 1995). The disturbance
74 could be intensive and cause a decrease of CO₂ consumption by weathering at about
75 73% due to acid precipitation in the Strengbach catchment (Vosges Mountains, France),
76 where is dominated by crystalline rocks (Amiotte-Suchet et al., 1995). This highlights
77 the importance of exploring anthropogenic impact on chemical weathering and CO₂

78 consumption under different background (e.g. lithology, climate, human activity
79 intensity, and basin scale) for better constraining and estimation of acid precipitation
80 effect on rock weathering. Asia, especially East Asia, is one of the world's major sulfur
81 and nitrogen emission areas. However, the effect of acid precipitation on silicate
82 weathering and associated CO₂ consumption has not been well evaluated in this area,
83 especially lack of quantitative studies.

84 Acid precipitation affected about 30% of the territory of China (Fig. 1), and the
85 seriously polluted areas are mainly located in the east, the south and the center of China,
86 where over 70% of the cities were suffering from acid rain (Zhang et al., 2007a; State
87 Environmental Protection Administration of China, 2009). Southeast coastal region of
88 China is one of the most developed and populated areas of this country, dominated by
89 Mesozoic magmatic rocks (mainly granite and volcanic rocks) in lithology. Meanwhile,
90 the southeast coastal area has become one of the three major acid rain areas in China
91 since the beginning of 1990s (Larssen et al., 1999). It is seriously impacted by acid rain,
92 with a volume-weighted mean value of pH lower than 4.5 for many years (Wang et al.,
93 2000; Larssen and Carmichael, 2000; Zhao, 2004; Han et al., 2006; Larssen et al., 2006;
94 Zhang et al., 2007a; Huang et al., 2008; Xu et al., 2011). Therefore, it is an ideal area
95 for evaluating silicate weathering and the associated acid rain effects. In the previous
96 work, we have recognized and discussed the importance of sulfuric acid on the rock
97 weathering and associated CO₂ consumption in the Qiantang river basin in this area
98 (Liu et al., 2016). However, it is difficult to infer the anthropogenic impact on chemical
99 weathering and CO₂ consumption in the whole southeast coastal area from the case

100 study of a single river basin, because of the variations on lithology, basin scale, runoff
101 and anthropogenic condition in the large acid deposition affected area. In this study, the
102 chemical and carbon isotope composition of river waters in this area were first
103 systematically investigated, in order to: (i) decipher the different sources of solutes and
104 to quantify their contributions to the dissolved loads; (ii) calculate silicate weathering
105 and associated CO₂ consumption rates; (iii) evaluate the effects of acid deposition on
106 rock weathering and CO₂ consumption flux in the whole southeast coastal river basins.

107 **2. Natural setting of study area**

108 Southeast coastal region of China, where the landscape is dominated by
109 mountainous and hilly terrain, lacks the conditions for developing large rivers. The
110 rivers in this region are dominantly small and medium-size drainage due to the
111 topographic limitation. Only 5 rivers in this region have length over 200 km and the
112 drainage area over 10,000 km², and they are: the Qiantangjiang (Qiantang) and the
113 Oujiang (Ou) in Zhejiang province, the Minjiang (Min) and the Jiulongjiang (Jiulong)
114 in Fujian province and the Hanjiang (Han) in Guangdong province from north to south
115 (Fig. 1). Rivers in this region generally flow eastward or southward and finally inject
116 into the East China Sea or the South China Sea (Fig. 1), and they are collectively named
117 as ‘Southeast Coastal Rivers’ (SECRs).

118 The Southeast Coastal Rivers Basin (SECRB) belongs to the warm and humid
119 subtropical oceanic monsoon climate. The mean annual temperature and precipitation
120 are 17-21°C and 1400-2000 mm, respectively. The precipitation mainly happens during
121 May to September, and the lowest and highest temperature often occurs in January and

122 July. This area is one of the most developed areas in China, with a population more than
123 190 million (mean density of ~ 470 individuals/km²), but the population mainly
124 concentrated in the coastal urban areas. The vegetation coverage of these river basins
125 is higher than 60%, mainly subtropical evergreen-deciduous broadleaf forest and
126 mostly distributing in mountains area. Cultivated land, and industries and cities are
127 mainly located in the plain areas and lower reach of these rivers.

128 Geologically, three regional-scale fault zones are distributed across the SECRB
129 region (Fig. 1). They are the sub-EW-trending Shaoxing-Jiangshan fault zone, the NE-
130 trending Zhenghe-Dapu fault zone, and the NE-trending Changle-Nanao fault zone
131 (Shu et al., 2009). These fault zones dominate the direction of the mountains ridgelines
132 and drainages, as well as the formation of the basins and bay. The Zhenghe-Dapu fault
133 zone is a boundary line of Caledonian uplift belt and Hercynian-Indosinian depression
134 zone. Mesozoic magmatic rocks are widespread in the southeast coastal region with a
135 total outcrop area at about 240,000 km². Over 90% of the Mesozoic magmatic rocks
136 are granitoids (granites and rhyolites) and their volcanic counterpart with minor
137 existence of basalts (Zhou et al., 2000, 2006; Bai et al., 2014). These crust-derived
138 granitic rocks are mainly formed in the Yanshanian stage, and may have been related to
139 multiple collision events between Cathaysia and Yangtze blocks and Pacific plate (Zhou
140 and Li, 2000; Xu et al., 2016). Among the major river basins, the proportions of
141 magmatic rocks outcrop are about 36% in the Qiantang catchment, over 80% in the Ou,
142 the Jiaoxi and the Jin catchments, and around 60% in the Min, the Jiulong, the Han and
143 the Rong catchments (Shi, 2014). The overlying Quaternary sediment in this area is

144 composed of brown-yellow siltstones but is rarely developed. The oldest basement
145 complex is composed of metamorphic rocks of greenschist and amphibolite facies.
146 Sedimentary rocks categories into two types, one is mainly composed by red elastic
147 rocks which cover more than 40,000 km² in the area; the other occurs as interlayers
148 within volcanic formations, including varicolored mudstones and sandstones. They are
149 mainly distributed on the west of Zhenghe-Dapu fault zone (FJBGRM, 1985; ZJBGMR,
150 1989; Shu et al., 2009).

151 **3. Sampling and analytical method**

152 A total of 121 water samples were collected from mainstream and tributaries of
153 the major rivers in the SECRB in July of 2010 in the high-flow period (sample number
154 and locations are shown in Fig. 1). For the river low reach samples, the sampling sites
155 were selected as far as possible from the tidal impacted area and the sampling were
156 conducted during low tide period (based on the daily tidal time,
157 <http://ocean.cnss.com.cn/>) in the sampling day. Besides, the salinity of the waters were
158 checked by salinometer (WS202, China) before sampling in the field. In addition, water
159 chemistry data were double checked to make sure that the river samples were not
160 contaminated by seawater. 2-L water samples were collected in the middle channel of
161 the rivers from bridges or ferries, or directly from the center of some shallow streams.
162 The lower reach sampling sites were selected distant away from the estuary to avoid
163 the influence of seawater. Temperature (T), pH and electrical conductivity (EC) were
164 measured in the field with a portable EC/pH meter (YSI-6920, USA). All of the water
165 samples for chemical analysis were filtered in field through 0.22 μm Millipore

166 membrane filter, and the first portion of the filtration was discarded to wash the
167 membrane and filter. One portion filtrate were stored directly in HDPE bottles for anion
168 analysis and another were acidified to $\text{pH} < 2$ with 6 M double sub-boiling distilled
169 HNO_3 for cation analysis. All containers were previously washed with high-purity HCl
170 and rinsed with Milli-Q 18.2 M Ω water.

171 Alkalinity was determined by phenolphthalein and methyl orange end point titration with
172 dilute HCl within 12 h after sampling. The HCl consumption volumes for phenolphthalein
173 and methyl orange end point titration were used to calculate the HCO_3^- . Cations (Na^+ , K^+ ,
174 Ca^{2+} and Mg^{2+}) were determined using Inductively Coupled Plasma Atomic Emission
175 Spectrometer (ICP-AES) (IRIS Intrepid II XSP, USA). Anions (Cl^- , F^- , NO_3^- and SO_4^{2-})
176 were analyzed by ionic chromatography (IC) (Dionex Corporation, USA). Dissolved
177 silica was determined by spectrophotometry with the molybdate blue method. Reagent
178 and procedural blanks were measured in parallel to the sample treatment, and
179 calibration curve was evaluated by quality control standards before, during and after
180 the analyses of each batch of samples. Measurement reproducibility was determined by
181 duplicated sample and standards, which showed $\pm 3\%$ precision for the cations and $\pm 5\%$
182 for the anions.

183 River water samples for carbon isotopic ratio ($\delta^{13}\text{C}$) of dissolved inorganic carbon
184 (DIC) measurements were collected in 150 ml glass bottles with air-tight caps and
185 preserved with HgCl_2 to prevent biological activity. The samples were kept refrigerated
186 until analysis. For the $\delta^{13}\text{C}$ measurements, the filtered samples were injected into glass
187 bottles with phosphoric acid. The CO_2 was then extracted and cryogenically purified

188 using a high vacuum line. $\delta^{13}\text{C}$ isotopic ratios were analyzed on Finnigen MAT-252
189 stable isotope mass spectrometer at the State Key Laboratory of Environmental
190 Geochemistry, Chinese Academy of Sciences. The results are expressed with reference
191 to VPDB, as follows:

$$192 \quad \delta^{13}\text{C} = [((^{13}\text{C}/^{12}\text{C})_{\text{sample}} / (^{13}\text{C}/^{12}\text{C})_{\text{standard}}) - 1] \times 1000 \quad (1)$$

193 The $\delta^{13}\text{C}$ measurement has an precision of 0.1‰. A number of duplicate samples
194 were measured and the results show that the differences were less than the range of
195 measurement accuracy.

196 **4. Results**

197 The major parameter and ion concentrations of samples are given in Table 1. The
198 pH values of water samples ranged from 6.50 to 8.24, with an average of 7.23. Total
199 dissolved solids (TDS) of water samples varied from 35.3 to 205 mg l^{-1} , with an average
200 of 75.2 mg l^{-1} . Compared with the major rivers in China, the average TDS was
201 significantly lower than the Changjiang (224 mg l^{-1} , Chetelat et al., 2008), the Huanghe
202 (557 mg l^{-1} , Fan et al., 2014) and the Zhujiang (190 mg l^{-1} , Zhang et al., 2007b).
203 However, the average TDS was comparable to the rivers draining silicate rock
204 dominated areas, e.g. the upper Ganjiang in Ganzhou, south China (63 mg l^{-1} , Ji and
205 Jiang, 2012), the Amur in north China (70 mg l^{-1} , Moon et al., 2009), the Xishui in
206 Hubei, central China (101 mg l^{-1} , Wu et al., 2013), and north Han river in South Korea
207 (75.5 mg l^{-1} , Ryu et al., 2008). Among the major rivers in the SECRB, the Qiantang had
208 the highest TDS value (averaging at 121 mg l^{-1}), and the Ou had the lowest TDS value
209 (averaging at 48.8 mg l^{-1}).

210 Major ion compositions are shown in the cation and anion ternary diagrams (Fig.
211 2a and b). In comparison with rivers (e.g. the Wujiang and Xijiang) draining carbonate
212 rocks dominated area (Han and Liu, 2004; Xu and Liu, 2010), these rivers in the SECRB
213 had distinctly higher proportions of Na^+ , K^+ , and dissolved SiO_2 . As shown in the Fig.
214 2, most samples had high Na^+ and K^+ proportions, with an average more than 50% (in
215 $\mu\text{mol l}^{-1}$) of the total cations, except for samples from the Qiantang. The concentrations
216 of Na^+ and K^+ ranged from 43.5 to 555 $\mu\text{mol l}^{-1}$ and 42.9 to 233 $\mu\text{mol l}^{-1}$, with average
217 values of 152 and 98 $\mu\text{mol l}^{-1}$, respectively. The concentrations of dissolved SiO_2 ranged
218 from 98.5 to 370 $\mu\text{mol l}^{-1}$, with an average of 212 $\mu\text{mol l}^{-1}$. Ca^{2+} and Mg^{2+} accounted
219 for about 38% and 11.6% of the total cation concentrations. HCO_3^- was the dominant
220 anion with concentrations ranging from 139 to 1822 $\mu\text{mol l}^{-1}$. On average, it comprised
221 60.6% (36-84.6%) of total anions on a molar unit basis, followed by SO_4^{2-} (14.6%), Cl^-
222 (13.1%) and NO_3^- (11.8%). The major ionic compositions indicate that water chemistry
223 of these rivers in the SECRB is controlled by silicate weathering. Meanwhile, it is also
224 influenced by carbonate weathering, especially for the Qiantang catchment.

225 The $\delta^{13}\text{C}$ of dissolved inorganic carbon in the rivers of the SECRB are also given
226 in Table 1. The $\delta^{13}\text{C}$ of the water samples showed a wide range, from -11.0‰ to -24.3‰
227 (average -19.4‰), and with a majority of samples falling into the range of -15 to -23‰.
228 The values are comparable to rivers draining Deccan Traps (Das et al., 2005).

229 **5. Discussion**

230 The dissolved solids in river water are commonly from atmospheric and
231 anthropogenic inputs and weathering of rocks within the drainage basin. It is necessary

232 to quantify the contribution of different sources to the dissolved loads before deriving
233 chemical weathering rates and associated CO₂ consumption.

234 *5.1 Atmospheric and anthropogenic inputs*

235 To evaluate atmospheric inputs to river waters, chloride is the most common used
236 reference. Generally, water samples that have the lowest Cl⁻ concentrations are
237 employed to correct the proportion of atmospheric inputs in a river system (Négrel et
238 al., 1993; Gaillardet et al., 1997; Viers et al., 2001; Xu and Liu, 2007). In pristine areas,
239 the concentration of Cl⁻ in river water is assumed to be entirely derived from the
240 atmosphere, provided that the contribution of evaporites is negligible (e.g. Stallard and
241 Edmond, 1981; Négrel et al., 1993). In the SECRB, the lowest Cl⁻ concentration was
242 mainly found in the headwater of each river. According to the geologic setting, no salt-
243 bearing rocks was found in these headwater area (FJBGRM, 1985; ZJBGMR, 1989). In
244 addition, these areas are mainly mountainous and sparsely populated. Therefore, we
245 assumed that the lowest Cl⁻ concentration of samples from the headwater of each major
246 river came entirely from atmosphere.

247 The proportion of atmosphere-derived ions in the river waters can then be
248 calculated by using the element/Cl ratios of the rain. Chemical compositions of rain in
249 the studied area have been reported at different sites, including Hangzhou, Jinhua,
250 Nanping, Fuzhou and Xiamen (Zhao, 2004; Zhang et al., 2007a; Huang et al., 2008;
251 Cheng et al., 2011; Xu et al., 2011) (Fig. 1). The volume-weighted mean concentration
252 of ions and Cl-normalized molar ratios are compiled in Table 2. According to this
253 procedure, 6.6-23.4% (averaging 14.3%) of total dissolved cations in the major rivers

254 of the SECRB originated from rain. Among the anions, SO_4^{2-} and NO_3^- in the rivers are
255 mainly from the atmospheric input, averaging at 73.2% for SO_4^{2-} and 75.8% for NO_3^- ,
256 respectively.

257 As one of the most developed and populated areas in China, the chemistry of river
258 waters in the SECRB could be significantly impacted by anthropogenic inputs. Cl^- ,
259 NO_3^- and SO_4^{2-} are commonly associated with anthropogenic sources and have been
260 used as tracers of anthropogenic inputs in watershed. High concentrations of Cl^- , NO_3^-
261 and SO_4^{2-} can be found at the lower reaches of rivers in the SECRB, and there is an
262 obvious increase after flowing through plain areas and cities. This tendency indicates
263 that river water chemistry is affected by anthropogenic inputs while passing through
264 the catchments. After correcting for the atmospheric contribution to river waters, the
265 following assumption is needed to quantitatively estimate the contributions of
266 anthropogenic inputs, which is that Cl^- originates from only atmospheric and
267 anthropogenic inputs, and the excess of atmospheric Cl^- is regarded to present
268 anthropogenic inputs and balanced by Na^+ .

269 *5.2 Chemical weathering inputs*

270 Water samples were plotted on a plot of Na-normalized molar ratios (Fig. 3). The
271 values of the world's large rivers (Gaillardet et al., 1999) are also shown in the figure.
272 A best correlations between elemental ratios were observed for $\text{Ca}^{2+}/\text{Na}^+$ vs. $\text{Mg}^{2+}/\text{Na}^+$
273 ($R^2 = 0.95$, $n = 120$) and $\text{Ca}^{2+}/\text{Na}^+$ vs. $\text{HCO}_3^-/\text{Na}^+$ ($R^2 = 0.98$, $n = 120$). The samples
274 cluster on a mixing line mainly between silicate and carbonate end-members, closer to
275 the silicate end-member, and with little evaporite contribution. This corresponds with

276 the rock type distributions in the SECRB. In addition, all water samples have equivalent
277 ratios of $(\text{Na}^+ + \text{K}^+)/\text{Cl}^-$ larger than one, indicating silicate weathering as the source of
278 Na^+ and K^+ rather than chloride evaporites dissolution.

279 The geochemical characteristics of the silicate and carbonate end-members can be
280 deduced from the correlations between elemental ratios and referred to literature data
281 for catchments with well-constrained lithology. After correction for atmospheric inputs,
282 the $\text{Ca}^{2+}/\text{Na}^+$, $\text{Mg}^{2+}/\text{Na}^+$ and $\text{HCO}_3^-/\text{Na}^+$ of the river samples ranged from 0.31 to 30,
283 0.16 to 6.7, and 1.1 to 64.2, respectively. According to the geological setting (Fig. 1),
284 there are some small rivers draining purely silicate areas in the SECRs drainage basins.
285 Based on the elemental ratios of these rivers, we assigned the silicate end-member for
286 this study as $\text{Ca}^{2+}/\text{Na}^+ = 0.41 \pm 0.10$, $\text{Mg}^{2+}/\text{Na}^+ = 0.20 \pm 0.03$ and $\text{HCO}_3^-/\text{Na}^+ = 1.7 \pm 0.6$. The
287 ratio of $(\text{Ca}^{2+} + \text{Mg}^{2+})/\text{Na}^+$ for silicate end-member was 0.61 ± 0.13 , which is close to the
288 silicate end-member of world rivers ($(\text{Ca}^{2+} + \text{Mg}^{2+})/\text{Na}^+ = 0.59 \pm 0.17$, Gaillardet et al.,
289 1999). Moreover, previous researches have documented the chemical composition of
290 rivers, such as the Amur and the Songhuajiang in North China, the Xishui in the lower
291 reaches of the Changjiang, and major rivers in South Korea (Moon et al., 2009; Liu et
292 al., 2013; Wu et al., 2013; Ryu et al., 2008; Shin et al., 2011). These river basins has
293 similar lithological setting with the study area, we could further validate the
294 composition of silicate end-member with their results. $\text{Ca}^{2+}/\text{Na}^+$ and $\text{Mg}^{2+}/\text{Na}^+$ ratios of
295 silicate end-member were reported for the Amur (0.36 and 0.22), the Songhuajiang
296 (0.44 ± 0.23 and 0.16), the Xishui (0.6 ± 0.4 and 0.32 ± 0.18), the Han (0.55 and 0.21) and
297 six major rivers in South Korea (0.48 and 0.20) in the studies above, well bracketing

298 our estimation for silicate end-member.

299 Whereas, some samples show high concentrations of Ca^{2+} , Mg^{2+} and HCO_3^- ,
300 indicating the contribution of carbonate weathering. The samples collected in the upper
301 reaches (Sample 12 and 13) of the Qiantang fall close to the carbonate end-member
302 documented for world's large rivers (Gaillardet et al., 1999). In the present study,
303 $\text{Ca}^{2+}/\text{Na}^+$ ratio of 0.41 ± 0.10 and $\text{Mg}^{2+}/\text{Na}^+$ ratio of 0.20 ± 0.03 for silicate end-member
304 are used to calculate the contribution of Ca^{2+} and Mg^{2+} from silicate weathering. Finally,
305 residual Ca^{2+} and Mg^{2+} are apportioned to carbonate weathering origin.

306 *5.3 Chemical weathering rate in the SECRBs*

307 Based on the above assumption, a forward model is employed to quantify the
308 relative contribution of the different sources to the rivers of the SECRB in this study.
309 (e.g. Galy and France-Lanord, 1999; Moon et al., 2007; Xu and Liu, 2007; 2010; Liu
310 et al., 2013). The calculated contributions of different reservoir to the total cationic
311 loads for major rivers and their main tributaries in the SECRB are presented in Fig. 4.
312 On average, the dissolved cationic loads of the rivers in the study area originate
313 dominantly from silicate weathering, which accounts for 39.5% (17.8-74.0%) of the
314 total cationic loads in molar unit. Carbonate weathering and anthropogenic inputs
315 account for 30.6% (3.9-62.0%) and 15.7% (0-41.1%), respectively. Contributions from
316 silicate weathering are high in the Ou (55.6%), the Huotong (54.5%), the Ao (48.3%)
317 and the Min (48.3%) river catchments, which are dominated by granitic and volcanic
318 bedrocks. In contrast, high contribution from carbonate weathering is observed in the
319 Qiantang (54.0%), the Jin (52.2%) and the Jiulong (44.8%) river catchments. The

320 results manifest the lithology control on river solutes of drainage basin.

321 The chemical weathering rate of rocks is estimated by the mass budget, basin area
322 and annual discharge (data from the Annual Hydrological Report P. R. China, 2010,
323 Table 3), expressed in $\text{t km}^{-2} \text{ a}^{-1}$. The silicate weathering rate (SWR) is calculated using
324 major cationic concentrations from silicate weathering and assuming that all dissolved
325 SiO_2 is derived from silicate weathering (Xu and Liu, 2010), as the equation below:

$$326 \quad \text{SWR} = ([\text{Na}]_{\text{sil}} + [\text{K}]_{\text{sil}} + [\text{Ca}]_{\text{sil}} + [\text{Mg}]_{\text{sil}} + [\text{SiO}_2]_{\text{riv}}) \times \text{discharge} / \text{area} \quad (2)$$

327 The assumption about Si could lead to overestimation of the silicate weathering
328 rate, as part of silica may come from dissolution of biogenic materials rather than the
329 weathering of silicate minerals (Millot et al., 2003; Shin et al., 2011). Thus, the cationic
330 silicate weathering rates (Cat_{sil}) were also calculated.

331 The carbonate weathering rate (CWR) is calculated based on the sum of Ca^{2+} ,
332 Mg^{2+} and HCO_3^- from carbonate weathering, with half of the HCO_3^- coming from
333 carbonate weathering being derived from the atmosphere CO_2 , as the equation below:

$$334 \quad \text{CWR} = ([\text{Ca}]_{\text{carb}} + [\text{Mg}]_{\text{carb}} + 1/2[\text{HCO}_3]_{\text{carb}}) \times \text{discharge} / \text{area} \quad (3)$$

335 The chemical weathering rate and flux are calculated for major rivers and their
336 main tributaries in the SECRB, and the results are shown in Table 3. Silicate and
337 carbonate weathering fluxes of these rivers (SWF and CWF) range from $0.02 \times 10^6 \text{ t a}^{-1}$
338 1 to $1.80 \times 10^6 \text{ t a}^{-1}$, and from $0.004 \times 10^6 \text{ t a}^{-1}$ to $1.74 \times 10^6 \text{ t a}^{-1}$, respectively. Among the
339 rivers, the Min has the highest silicate weathering flux, and the Qiantang has the highest
340 carbonate weathering flux. On the whole SECRB scale, $3.95 \times 10^6 \text{ t a}^{-1}$ and $4.09 \times 10^6 \text{ t}$
341 a^{-1} of dissolved solids originating from silicate and carbonate weathering, respectively,

342 are transported into the East and South China Sea by rivers in this region. Compared
343 with the largest three river basins (the Changjiang, the Huanghe and the Xijiang) in
344 China, the flux of silicate weathering calculated for the SECRB is lower than the
345 Changjiang ($9.5 \times 10^6 \text{ t a}^{-1}$, Gaillardet et al. 1999), but higher than the Huanghe
346 ($1.52 \times 10^6 \text{ t a}^{-1}$, Fan et al., 2014) and the Xijiang ($2.62 \times 10^6 \text{ t a}^{-1}$, Xu and Liu, 2010).

347 The silicate and carbonate chemical weathering rates for these river watersheds
348 were $14.2\text{-}35.8 \text{ t km}^{-2} \text{ a}^{-1}$ and $1.8\text{-}52.1 \text{ t km}^{-2} \text{ a}^{-1}$, respectively. The total rock weathering
349 rate (TWR) for the whole SECRB is $48.1 \text{ t km}^{-2} \text{ a}^{-1}$, higher than the world average (24
350 $\text{ t km}^{-2} \text{ a}^{-1}$, Gaillardet et al., 1999). The cationic silicate weathering rates (Cat_{sil}) ranges
351 from 4.7 to $12.0 \text{ t km}^{-2} \text{ a}^{-1}$ for the river watersheds in the SECRB, averaging at 7.8 t km^{-2}
352 a^{-1} . Furthermore, a good linear correlation ($R^2 = 0.77$, $n = 28$) is observed between the
353 Cat_{sil} and runoff (Fig. 5), indicating that silicate weathering rates is controlled by runoff
354 as documented in previous researches (e.g., Bluth and Kump, 1994; Gaillardet et al.,
355 1999; Millot et al., 2002; Oliva et al., 2003; Wu et al., 2013; Pepin et al., 2013).

356 *5.4 CO₂ consumption and the role of sulfuric acid*

357 To calculate atmospheric CO₂ consumption by silicate weathering (CSW) and by
358 carbonate weathering (CCW), a charge-balanced state between rock chemical
359 weathering-derived alkalinity and cations was assumed (Roy et al., 1999).

$$360 \quad [\text{CO}_2]_{\text{CSW}} = [\text{HCO}_3]_{\text{CSW}} = [\text{Na}]_{\text{sil}} + [\text{K}]_{\text{sil}} + 2[\text{Ca}]_{\text{sil}} + 2[\text{Mg}]_{\text{sil}} \quad (4)$$

$$361 \quad [\text{CO}_2]_{\text{CCW}} = [\text{HCO}_3]_{\text{CCW}} = [\text{Ca}]_{\text{carb}} + [\text{Mg}]_{\text{carb}} \quad (5)$$

362 The calculated CO₂ consumption rates by chemical weathering for the rivers in
363 SECRB are shown in Table 3. CO₂ consumption rates by carbonate and silicate

364 weathering are from 17.9 to $530 \times 10^3 \text{ mol km}^{-2} \text{ a}^{-1}$ (averaging at $206 \times 10^3 \text{ mol km}^{-2} \text{ a}^{-1}$)
365 and from 167 to $460 \times 10^3 \text{ mol km}^{-2} \text{ a}^{-1}$ (averaging at $281 \times 10^3 \text{ mol km}^{-2} \text{ a}^{-1}$) for major
366 river catchments in the SECRB. The CO_2 consumption rates by silicate weathering in
367 the SECRB are higher than that of major rivers in the world and China, such as the
368 Amazon ($174 \times 10^3 \text{ mol km}^{-2} \text{ a}^{-1}$, Mortatti and Probst, 2003), the Mississippi and the
369 Mackenzie (66.8 and $34.1 \times 10^3 \text{ mol km}^{-2} \text{ a}^{-1}$, Gaillardet et al., 1999), the Changjiang
370 ($112 \times 10^3 \text{ mol km}^{-2} \text{ a}^{-1}$, Chetelat et al., 2008), the Huanghe ($35 \times 10^3 \text{ mol km}^{-2} \text{ a}^{-1}$, Fan et
371 al., 2014), the Xijiang ($154 \times 10^3 \text{ mol km}^{-2} \text{ a}^{-1}$, Xu and Liu, 2010), the Longchuanjiang
372 ($173 \times 10^3 \text{ mol km}^{-2} \text{ a}^{-1}$, Li et al., 2011) and the Mekong ($191 \times 10^3 \text{ mol km}^{-2} \text{ a}^{-1}$, Li et al.,
373 2014) and three large rivers in eastern Tibet (103 - $121 \times 10^3 \text{ mol km}^{-2} \text{ a}^{-1}$, Noh et al.,
374 2009), the Hanjiang in central China ($120 \times 10^3 \text{ mol km}^{-2} \text{ a}^{-1}$, Li et al., 2009) and the
375 Sonhuajiang in north China ($66.6 \times 10^3 \text{ mol km}^{-2} \text{ a}^{-1}$, Liu et al., 2013). The high CO_2
376 consumption rates by silicate weathering in the SECRB could be attributed to extensive
377 distribution of silicate rocks, high runoff, favorable climatic conditions. The regional
378 fluxes of CO_2 consumption by silicate and carbonate weathering is about $47.9 \times 10^9 \text{ mol}$
379 a^{-1} ($0.57 \times 10^{12} \text{ g C a}^{-1}$) and $41.9 \times 10^9 \text{ mol a}^{-1}$ ($0.50 \times 10^{12} \text{ g C a}^{-1}$) in the whole SECRB.

380 However, in addition to CO_2 , the anthropogenic sourced proton (e.g. H_2SO_4 and
381 HNO_3) is well documented as significant proton providers in rock weathering process
382 (Galy and France-Lanord, 1999; Karim and Veizer, 2000; Yoshimura et al., 2001; Han
383 and Liu, 2004; Spence and Telmer, 2005; Lerman and Wu, 2006; Xu and Liu 2007;
384 2010; Perrin et al., 2008; Gandois et al., 2011). Sulfuric acid can be generated by natural
385 oxidation of pyrite and anthropogenic emissions of SO_2 from coal combustion and

386 subsequently dissolve carbonate and silicate minerals. The riverine nitrate in a
387 watershed can be derived from atmospheric deposition, synthetic fertilizers, microbial
388 nitrification, sewage and manure, etc. (e.g. Kendall 1998). Although it is difficult to
389 determine the sources of nitrate in river waters, we can at least simply assume that
390 nitrate from acid deposition is one of the proton providers. The consumption of CO₂ by
391 rock weathering would be overestimated if H₂SO₄ and HNO₃ induced rock weathering
392 was ignored (Spence and Telmer, 2005; Xu and Liu, 2010; Shin et al., 2011; Gandois
393 et al., 2011). Thus, the role of the anthropogenic sourced protons plays on the chemical
394 weathering is crucial for an accurate estimation of CO₂ consumption by rock
395 weathering.

396 Rapid economic growth and increased energy needs have result in severe air
397 pollution problems in many areas of China, indicated by the high levels of mineral acids
398 (predominately sulfuric) observed in precipitation (Lassen and Carmichael, 2000; Pan
399 et al., 2013; Liu et al., 2016). The national SO₂ emissions in 2010 reached to 30.8
400 Tg/year (Lu et al., 2011). Previous study documented that fossil fuel combustion
401 accounts for the dominant sulfur deposition (~77%) in China (Liu et al., 2016). The wet
402 deposition rate of nitrogen is the highest in peaked over the central and south China,
403 with mean value of 20.2, 18.2 and 25.8 kg N ha⁻¹ yr⁻¹ in Zhejiang, Fujian and
404 Guangdong province, respectively (Lu and Tian, 2007). Current sulfur and nitrogen
405 depositions in the southeast coastal region are still among the highest in China (Fang et
406 al., 2013; Cui et al., 2014; Liu et al., 2016).

407 The involvement of protons originating from H₂SO₄ and HNO₃ in the river waters

408 can be illustrated by the stoichiometry between cations and anions, shown in Fig. 6. In
409 the rivers of the SECRB, the sum cations released by silicate and carbonate weathering
410 could not be balanced by HCO_3^- only (Fig. 6a), but were almost balanced by the sum
411 of HCO_3^- and SO_4^{2-} and NO_3^- (Fig. 6b). This implies that H_2CO_3 and H_2SO_4 and HNO_3
412 are the potential erosion agents in chemical weathering in the SECRB. The $\delta^{13}\text{C}$ values
413 of the water samples showed a wide range, from -11.0‰ to -24.3‰, with an average of
414 -19.4‰. The $\delta^{13}\text{C}$ from soil is governed by the relative contribution from C_3 and C_4
415 plant (Das et al., 2005). The studied areas have subtropical temperatures and humidity,
416 and thus C_3 processes are dominant. The $\delta^{13}\text{C}$ of soil CO_2 is derived primarily from
417 $\delta^{13}\text{C}$ of organic material which typically has a value of -24 to -34‰, with an average of
418 -28‰ (Faure, 1986). According to previous studies, the average value for C_3 trees and
419 shrubs are from -24.4 to -30.5‰, and most of them are lower than -28‰ in south China
420 (Chen et al., 2005; Xiang, 2006; Dou et al., 2013). After accounting for the isotopic
421 effect from diffusion of CO_2 from soil, the resulted $\delta^{13}\text{C}$ (from the terrestrial C_3 plant
422 process) should be \sim -25‰ (Cerling et al., 1991). This mean DIC derived from silicate
423 weathering by carbonic acid (100% from soil CO_2) would yield a $\delta^{13}\text{C}$ value of -25‰.
424 Carbonate rocks are generally derived from marine system and, typically, have $\delta^{13}\text{C}$
425 value close to zero (Das et al., 2005). Thus, the theoretical $\delta^{13}\text{C}$ value of DIC derived
426 from carbonate weathering by carbonic acid (50% from soil CO_2 and 50% from
427 carbonate rocks) is -12.5‰. DIC derived from carbonate weathering by sulfuric acid
428 are all from carbonate rocks, thus the $\delta^{13}\text{C}$ of the DIC would be 0‰. Based on the above
429 discussion, sources of riverine DIC from different end-members in the SECRB were

430 plotted in Fig. 7. Most water samples drift away from the three endmember mixing area
431 (carbonate and silicate weathering by carbonic acid and carbonate weathering by
432 sulfuric acid) and towards the silicate weathering by sulfuric and nitric acid area, clearly
433 illustrating the effect of the anthropogenic sourced protons on silicate weathering in the
434 SECRB.

435 Considering the H₂SO₄ and HNO₃ effect on chemical weathering, CO₂
436 consumption by silicate weathering can be determined from the equation below (Moon
437 et al., 2007; Ryu et al., 2008; Shin et al., 2011):

$$438 \quad [\text{CO}_2]_{\text{SSW}} = [\text{Na}]_{\text{sil}} + [\text{K}]_{\text{sil}} + 2[\text{Ca}]_{\text{sil}} + 2[\text{Mg}]_{\text{sil}} - \gamma \times [2\text{SO}_4 + \text{NO}_3]_{\text{atmos}} \quad (6)$$

439 Where γ is calculated by $\text{cation}_{\text{sil}} / (\text{cation}_{\text{sil}} + \text{cation}_{\text{carb}})$.

440 Based on the calculation in section 5.1, SO₄²⁻ and NO₃⁻ in river waters were mainly
441 derived from atmospheric input. Assuming SO₄²⁻ and NO₃⁻ in river waters derived from
442 atmospheric input (after correction for sea-salt contribution) are all from acid
443 precipitation, CO₂ consumption rates by silicate weathering (SSW) are estimated
444 between 55×10³ mol km⁻² a⁻¹ and 286×10³ mol km⁻² a⁻¹ for major river watersheds in
445 the SECRB. For the whole SECRB, the actual CO₂ consumption rates by silicate is
446 191×10³ mol km⁻² a⁻¹ when the effect of H₂SO₄ and HNO₃ is considered. The flux of
447 CO₂ consumption is overestimated by 16.1×10⁹ mol a⁻¹ (0.19×10¹² g C a⁻¹) due to the
448 involvement of H₂SO₄ and HNO₃ from acid precipitation, accounting for approximately
449 33.6% of total CO₂ consumption flux by silicate weathering in the SECRB. It highlights
450 the fact that the drawdown of atmospheric CO₂ by silicate weathering can be
451 significantly overestimated if acid deposition is ignored in long-term perspectives. The

452 result quantitatively shows that anthropogenic activities can significantly affect rock
453 weathering and associated atmospheric CO₂ consumption. The quantification of this
454 effect needs to be well evaluated in Asian and globally within the current and future
455 human activity background.

456 It is noticeable that the chemical weathering and associated CO₂ consumption rates
457 for the study area were calculated by the river water geochemistry of high-flow season.
458 As a subtropical monsoon climate area, the river water of the southeast coastal rivers is
459 mainly recharged by rain, and the amount of precipitation in high-flow season accounts
460 for more than 70% of the annual precipitation in the area. The processes in low-flow
461 season might be different for some extent. It is worth the further efforts to investigate
462 the hydrology and temperature effect on weathering rate and flux, as well as on the
463 anthropogenic impact evaluation in different climate regime and hydrology season.

464 **6. Conclusions**

465 River waters in the southeast coastal region of China are characterized by high
466 proportions of Na⁺, K⁺ and dissolved SiO₂, indicating the water chemistry of the rivers
467 in the SECRB is mainly controlled by silicate weathering. The dissolved cationic loads
468 of the rivers in the study area originate dominantly from silicate weathering, which
469 accounts for 39.5% (17.8-74.0%) of the total cationic loads. Carbonate weathering,
470 atmospheric and anthropogenic inputs account for 30.6%, 14.3% and 15.7%,
471 respectively. Meanwhile, more than 70% of SO₄²⁻ and NO₃⁻ in the river waters derived
472 from atmospheric input. The chemical weathering rate of silicates and carbonates for
473 the whole SECRB are estimated to be approximately 23.7 and 24.5 t km⁻² a⁻¹. About

474 $8.04 \times 10^6 \text{ t a}^{-1}$ of dissolved solids originating from rock weathering are transported into
475 the East and South China Sea by these rivers in the SECRB. With the assumption that
476 all the protons involved in the weathering reaction are provided by carbonic acid, the
477 CO_2 consumption rates by silicate and carbonate weathering are 287 and $251 \times 10^3 \text{ mol}$
478 $\text{km}^{-2} \text{ a}^{-1}$, respectively. However, both water chemistry and carbon isotope data provide
479 evidence that sulfuric and nitric acid from acid precipitation serves as significant agents
480 during chemical weathering. Considering the effect of sulfuric and nitric acid, the CO_2
481 consumption rate by silicate weathering for the SECRB are $191 \times 10^3 \text{ mol km}^{-2} \text{ a}^{-1}$.
482 Therefore, the CO_2 consumption flux would be overestimated by $16.1 \times 10^9 \text{ mol a}^{-1}$
483 ($0.19 \times 10^{12} \text{ g C a}^{-1}$) in the SECRB if the effect of sulfuric and nitric acid is ignored. This
484 work illustrates that anthropogenic disturbance by acid precipitation has profound
485 impact on CO_2 sequestration by rock weathering.

486 **Acknowledgements.** This work was financially supported by the Strategic Priority
487 Research Program of Chinese Academy of Sciences, Grant No. XDB (Grant No.
488 26000000), and Natural Science Foundation of China (Grant No. 41673020, 91747202,
489 41772380 and 41730857).

490 **References:**

491 Amiotte-Suchet, P., Probst, A. Probst, J.-L., Influence of acid rain on CO_2 consumption
492 by rock weathering: local and global scales. *Water Air Soil Pollut.* 85, 1563-1568,
493 1995.

494 Amiotte-Suchet, P., Probst, J.-L. Ludwig, W., Worldwide distribution of continental
495 rock lithology: implications for the atmospheric/soil CO_2 uptake by continental

496 weathering and alkalinity river transport to the oceans. *Global Biogeochem.*
497 *Cycles* 17, 1038-1052, 2003.

498 Bai, H., Song, L.S., Xia, W.P., Prospect analysis of hot dry rock (HDR) in Eastern part
499 of Jiangxi province, *Coal Geol. China* 26, 41-44. (In Chinese), 2014.

500 Berner, R.A., Caldeira, K., The need for mass balance and feedback in the geochemical
501 carbon cycle. *Geology* 25, 955-956, 1997.

502 Bluth, G.J.S., Kump, L.R., Lithological and climatological controls of river chemistry.
503 *Geochim. Cosmochim. Acta* 58, 2341-2359, 1994.

504 Brantley, S.L., Lebedeva, M., Learning to read the chemistry of regolith to understand
505 the Critical Zone. *Annual Review of Earth and Planetary Sciences*, 39: 387-416,
506 2011.

507 Calmels, D., Gaillardet, J., Brenot, A., France-Lanord, C., Sustained sulfide oxidation
508 by physical erosion processes in the Mackenzie River basin: climatic perspectives.
509 *Geology* 35, 1003-1006, 2007.

510 Calmels, D., Galy, A., Hovius, N., Bickle, M., West, A.J., Chen, M.-C., Chapman, H.,
511 Contribution of deep groundwater to the weathering budget in a rapidly eroding
512 mountain belt, Taiwan. *Earth Planet. Sci. Lett.* 303, 48-58, 2011.

513 Cerling, T.E., Solomon, D.K., Quade, J., Bownman, J.R., On the isotopic composition
514 of soil CO₂. *Geochim. Cosmochim. Acta* 55, 3403–3405, 1991.

515 Chen, Q., Shen, C., Sun, Y., Peng, S., Yi, W., Li Z., Jiang, M., Spatial and temporal
516 distribution of carbon isotopes in soil organic matter at the Dinghushan Biosphere
517 Reserve, South China. *Plant and Soil*, 273: 115–128, 2005.

518 Cheng, Y., Liu, Y., Huo, M., Sun, Q., Wang, H., Chen, Z., Bai, Y., Chemical
519 characteristics of precipitation at Nanping Mangdang Mountain in eastern China
520 during spring. *J. Environ. Sci.* 23, 1350-1358, 2011.

521 Chetelat, B., Liu, C., Zhao, Z., Wang, Q., Li, S., Li, J., Wang, B., Geochemistry of the
522 dissolved load of the Changjiang Basin rivers: anthropogenic impacts and
523 chemical weathering. *Geochim. Cosmochim. Acta* 72, 4254-4277, 2008.

524 Cui, J., Zhou, J., Peng, Y., He, Y., Yang, H., Mao, J., Atmospheric wet deposition of
525 nitrogen and sulfur to a typical red soil agroecosystem in Southeast China during
526 the ten-year monsoon seasons (2003-2012). *Atmos. Environ.* 82, 121-129, 2014.

527 Das, A., Krishnaswami, S., Sarin, M.M., Pande, K., Chemical weathering in the Krishna
528 Basin and Western Ghats of the Deccan Traps, India: Rates of basalt weathering
529 and their controls. *Geochim. Cosmochim. Acta* 69(8), 2067-2084, 2005.

530 Dou, X., Deng, Q., Li, M., Wang, W., Zhang, Q., Cheng, X., Reforestation of *Pinus*
531 *massoniana* alters soil organic carbon and nitrogen dynamics in eroded soil in
532 south China. *Ecological Engineering* 52, 154-160, 2013.

533 Edmond, J.M., Palmer, M.R., Measures, C.I., Grant, B., Stallard, R.F., The fluvial
534 geochemistry and denudation rate of the Guayana Shield in Venezuela, Colombia,
535 and Brazil. *Geochim. Cosmochim. Acta* 59, 3301-3325, 1995.

536 Fan, B.L., Zhao, Z.Q., Tao, F.X., Liu, B.J., Tao, Z.H., Gao, S., He, M.Y., Characteristics
537 of carbonate, evaporite and silicate weathering in Huanghe River basin: A
538 comparison among the upstream, midstream and downstream. *J. Asian Earth Sci.*
539 96, 17-26, 2014.

540 Fang, Y., Wang, X., Zhu, F., Wu, Z., Li, J., Zhong, L., Chen, D., Yoh, M., Three-decade
541 changes in chemical composition of precipitation in Guangzhou city, southern
542 China: has precipitation recovered from acidification following sulphur dioxide
543 emission control? *Tellus B* 65, 1-15, 2013.

544 Faure, G., *Principles of Isotope Geology*. Wiley, Toronto, pp. 492-493, 1986.

545 FJBGMR: Fujian Bureau of Geology and Mineral Resources, *Regional Geology of*
546 *Fujian Province*. Geol. Publ. House, Beijing, p. 671 (in Chinese with English
547 abstract), 1985.

548 Gaillardet, J., Dupré, B., Allègre, C.J., Négrel, P., Chemical and physical denudation in
549 the Amazon River basin. *Chem. Geol.* 142, 141-173, 1997.

550 Gaillardet, J., Dupré, B., Louvat, P., Allegre, C.J., Global silicate weathering and CO₂
551 consumption rates deduced from the chemistry of large rivers. *Chem. Geol.* 159,
552 3-30, 1999.

553 Galy, A., France-Lanord, C., Weathering processes in the Ganges-Brahmaputra basin
554 and the riverine alkalinity budget. *Chem. Geol.* 159, 31-60, 1999.

555 Gandois, L., Perrin, A.-S., Probst, A., Impact of nitrogenous fertilizer-induced proton
556 release on cultivated soils with contrasting carbonate contents: A column
557 experiment. *Geochim. Cosmochim. Acta* 75, 1185-1198, 2011.

558 Gislason, S.R., Arnorsson, S., Armannsson, H., Chemical weathering of basalt in
559 southwest Iceland: effects of runoff, age of rocks and vegetative/glacial cover.
560 *Am. J. Sci.* 296, 837-907, 1996.

561 Han, G., Liu, C.Q., Water geochemistry controlled by carbonate dissolution: a study of

562 the river waters draining karst-dominated terrain, Guizhou Province, China.
563 Chem. Geol. 204, 1-21, 2004.

564 Han, Z.W., Ueda, H., Sakurai, T., Model study on acidifying wet deposition in East Asia
565 during wintertime. Atmos. Environ. 40, 2360-2373, 2006.

566 Hartmann, J., Jansen, N., Dürr, H.H., Kempe, S., Köhler, P., Global CO₂ consumption
567 by chemical weathering: what is the contribution of highly active weathering
568 regions? Global Planet. Change 69, 185-194, 2009.

569 Huang, K., Zhuang, G., Xu, C., Wang Y., Tang A., The chemistry of the severe acidic
570 precipitation in Shanghai, China. Atmos. Res. 89, 149-160, 2008.

571 Huh, Y.S., Chemical weathering and climate - a global experiment: a review. Geosci. J.
572 7, 277-288, 2003.

573 Hydrological data of river basins in Zhejiang, Fujian province and Taiwan region,
574 Annual Hydrological Report P. R. China, 2010, Vol (7) (in Chinese)

575 Ji, H., Jiang, Y., Carbon flux and C, S isotopic characteristics of river waters from a
576 karstic and a granitic terrain in the Yangtze River system. J. Asian Earth Sci. 57,
577 38-53, 2012.

578 Karim, A., Veizer, H.E., Weathering processes in the Indus River Basin: implication
579 from riverine carbon, sulphur, oxygen and strontium isotopes. Chem. Geol. 170,
580 153-177, 2000.

581 Kendall, C., Tracing nitrogen sources and cycling in catchments. In: Kendall, C., &
582 McDonnell, J.J., (Eds) Isotope Tracers in Catchment Hydrology. Elsevier,
583 Amsterdam, 1998.

584 Kump, L.R., Brantley, S.L., Arthur, M.A., Chemical weathering, atmospheric CO₂ and
585 climate. *Ann. Rev. Earth Planet. Sci.* 28, 611-667, 2000.

586 Larssen, T., Carmichael, G.R., Acid rain and acidification in China: the importance of
587 base cation deposition. *Environ. Poll.* 110, 89-102, 2000.

588 Larssen, T., Lydersen, E., Tang, D., He, Y., Gao, J., Liu, H., Duan, L., Seip, H.M., Acid
589 rain in China. *Environ. Sci. Technol.* 40, 418-425, 2006.

590 Lerman, A., Wu, L., CO₂ and sulfuric acid controls of weathering and river water
591 composition. *J. Geochem. Explor.* 88, 427-430, 2006.

592 Lerman, A., Wu, L., Mackenzie, F.T., CO₂ and H₂SO₄ consumption in weathering and
593 material transport to the ocean, and their role in the global carbon balance. *Mar.*
594 *Chem.* 106, 326-350, 2007.

595 Li, S., Bush, R.T., Changing fluxes of carbon and other solutes from the Mekong River.
596 *Sci. Rep.* 5, 16005, 2015.

597 Li, S.Y., Lu, X.X., Bush, R.T., Chemical weathering and CO₂ consumption in the Lower
598 Mekong River. *Sci. Total Environ.* 472, 162-177, 2014.

599 Li, S.Y., Lu, X.X., He, M., Zhou, Y., Bei, R., Li, L., Zieglera, A.D., Major element
600 chemistry in the Upper Yangtze River: a case study of the Longchuanjiang River.
601 *Geomorphology* 129, 29-42, 2011.

602 Li, S.Y., Xu, Z.F., Wang, H., Wang, J.H., Zhang, Q.F., Geochemistry of the upper Han
603 River basin, China. 3: anthropogenic inputs and chemical weathering to the
604 dissolved load. *Chem. Geol.* 264, 89-95, 2009.

605 Liu, B., Liu, C.-Q., Zhang, G., Zhao, Z.-Q., Li, S.-L., Hu, J., Ding, H., Lang, Y.-C., Li.,

606 X.-D., Chemical weathering under mid- to cool temperate and monsoon-
607 controlled climate: A study on water geochemistry of the Songhuajiang River
608 system, northeast China. *Appl. Geochem.* 31, 265-278, 2013.

609 Liu, L., Zhang, X., Wang, S., Zhang, W., Lu, X., Bulk sulfur (S) deposition in China.
610 *Atmos. Environ.*, 135, 41-49, 2016.

611 Liu, W., Shi, C., Xu, Z., Zhao, T., Jiang, H., Liang, C., Zhang, X., Zhou, Li., Yu, C.,
612 Water geochemistry of the Qiantangjiang River, East China: Chemical weathering
613 and CO₂ consumption in a basin affected by severe acid deposition. *J.Asian Earth*
614 *Sci.*, 127, 246-256, 2016.

615 Lu, C., Tian, H., Spatial and temporal patterns of nitrogen deposition in China:
616 Synthesis of observational data. *J. Geophys. Res.* 112, D22S05, 2007.

617 Lu, Z., Zhang, Q., Streets, D.G., Sulfur dioxide and primary carbonaceous aerosol
618 emissions in China and India, 1996e2010. *Atmos. Chem. Phys.* 11, 9839-9864,
619 2011.

620 Millot, R., Gaillardet, J., Dupré, B., Allègre, C.J., Northern latitude chemical
621 weathering rates: clues from the Mackenzie River Basin, Canada. *Geochim.*
622 *Cosmochim. Acta* 67, 1305-1329, 2003.

623 Millot, R., Gaillardet, J., Dupré, B., Allègre, C.J., The global control of silicate
624 weathering rates and the coupling with physical erosion: new insights from rivers
625 of the Canadian Shield. *Earth Planet. Sci. Lett.* 196, 83-98, 2002.

626 Ministry of Environmental Protection of China, 2009. China Environmental Quality
627 Report 2008. China Environmental Sciences Press, Beijing. In Chinese.

628 Moon, S., Chamberlain, C.P., Hilley, G.E., New estimates of silicate weathering rates
629 and their uncertainties in global rivers. *Geochim. Cosmochim. Acta* 134, 257-274,
630 2014.

631 Moon, S., Huh, Y., Qin, J., van Pho, N., Chemical weathering in the Hong (Red) River
632 basin: Rates of silicate weathering and their controlling factors. *Geochim.*
633 *Cosmochim. Acta* 71, 1411-1430, 2007.

634 Moon, S., Huh, Y., Zaitsev, A., Hydrochemistry of the Amur River: Weathering in a
635 Northern Temperate Basin. *Aquat. Geochem.*, 15, 497-527, 2009.

636 Mortatti, J., Probst, J.L., Silicate rock weathering and atmospheric/soil CO₂ uptake in
637 the Amazon basin estimated from river water geochemistry: seasonal and spatial
638 variations. *Chem. Geol.* 197, 177-196, 2003.

639 Négrel, P., Allègre, C.J., Dupré, B., Lewin, E., Erosion sources determined by inversion
640 of major and trace element ratios and strontium isotopic ratios in river water: the
641 Congo Basin Case. *Earth Planet. Sci. Lett.* 120, 59-76, 1993.

642 Noh, H., Huh, Y., Qin, J., Ellis, A., Chemical weathering in the Three Rivers region of
643 Eastern Tibet. *Geochim. Cosmochim. Acta* 73, 1857-1877, 2009.

644 Oliva, P., Viers, J., Dupré B., Chemical weathering in granitic environments. *Chem.*
645 *Geol.* 202, 225-256, 2003.

646 Pan, Y., Wang, Y., Tang, G., Wu, D., Spatial distribution and temporal variations of
647 atmospheric sulfur deposition in Northern China: insights into the potential
648 acidification risks. *Atmos. Chem. Phys.* 13, 1675-1688, 2013.

649 Pepin, E., Guyot, J.L., Armijos, E., Bazan, H., Fraizy, P., Moquet, J.S., Noriega, L.,

650 Lavado, W., Pombosa, R. Vauchel, P., Climatic control on eastern Andean
651 denudation rates (Central Cordillera from Ecuador to Bolivia). *J. S. Am. Earth*
652 *Sci.* 44, 85-93, 2013.

653 Perrin, A.-S., Probst, A., Probst, J.-L., Impact of nitrogenous fertilizers on carbonate
654 dissolution in small agricultural catchments: Implications for weathering CO₂
655 uptake at regional and global scales. *Geochim, Cosmochim. Acta* 72, 3105-3123,
656 2008.

657 Probst, A., Gh'mari, A.El., Aubert, D., Fritz, B., McNutt, R., Strontium as a tracer of
658 weathering processes in a silicate catchment polluted by acid atmospheric inputs,
659 Strengbach, France. *Chem. Geol.* 170, 203-219, 2000.

660 Raymo, M.E., Ruddiman, W.F., Tectonic forcing of late Cenozoic climate. *Nature* 359,
661 117-122, 1992.

662 Raymond, P. A., Oh, N.H., Turner, R.E., Broussard, W., Anthropogenically enhanced
663 fluxes of water and carbon from the Mississippi River. *Nature* 451, 449-452, 2008.

664 Regnier, P., Friedlingstein, P., Ciais, P., Mackenzie, F.T.,...Thullner. M., Anthropogenic
665 perturbation of the carbon fluxes from land to ocean. *Nature Geosci.* 6, 597-607.
666 2013.

667 Reuss, J.O., Cosby, B.J., Wright, R.F., Chemical processes governing soil and water
668 acidification. *Nature* 329, 27-32, 1987.

669 Roy, S., Gaillardet, J., Allègre, C.J., Geochemistry of dissolved and suspended loads of
670 the Seine river, France: anthropogenic impact, carbonate and silicate weathering.
671 *Geochim. Cosmochim. Acta* 63, 1277-1292, 1999.

672 Ryu, J.S., Lee, K.S., Chang, H.W., Shin, H.S., Chemical weathering of carbonates and
673 silicates in the Han River basin, South Korea. *Chem. Geol.* 247, 66-80, 2008.

674 Semhi, K., Amiotte Suchet, P., Clauer, N., Probst, J.-L., Impact of nitrogen fertilizers
675 on the natural weathering-erosion processes and fluvial transport in the Garonne
676 basin. *Appl. Geochem.* 15 (6), 865-874, 2000.

677 Shi, C., Chemical characteristics and weathering of rivers in the Coast of Southeast
678 China (PhD Thesis). Institute of Geology and Geophysics, Chinese academy of
679 sciences, Beijing, China. pp, 1-100 (in Chinese with English abstract), 2014.

680 Shin, W.-J., Ryu, J.-S., Park, Y., Lee, K.-S., Chemical weathering and associated CO₂
681 consumption in six major river basins, South Korea. *Geomorphology* 129, 334-
682 341, 2011.

683 Shu, L.S., Zhou, X.M., Deng, P., Wang, B., Jiang, S.Y., Yu, J.H., Zhao, X.X., Mesozoic
684 tectonic evolution of the Southeast China Block: New insights from basin
685 analysis. *J. Asian Earth Sci.* 34(3), 376-391, 2009.

686 Spence, J., Telmer, K., The role of sulfur in chemical weathering and atmospheric CO₂
687 fluxes: Evidence from major ions, $\delta^{13}\text{C}_{\text{DIC}}$, and $\delta^{34}\text{S}_{\text{SO}_4}$ in rivers of the Canadian
688 Cordillera. *Geochim. Cosmochim. Acta* 69, 5441-5458, 2005.

689 Stallard, R.F., Edmond, J.M., Geochemistry of the Amazon. Precipitation chemistry and
690 the marine contribution to the dissolved load at the time of peak discharge. *J.*
691 *Geophys. Res.*, 86, 9844-9858, 1981.

692 U.S. Nat. Res. Council Comm., Basic Research Opportunities in Earth Science.
693 Washington, DC: Nat. Acad. 154 pp., 2001.

694 Viers, J., Dupré, B., Braun, J.J., Freydier, R., Greenberg, S., Ngoupayou, J.N.,
695 Nkamdjou, L.S., Evidence for non-conservative behavior of chlorine in humid
696 tropical environments. *Aquat. Geochem.* 7, 127-154, 2001.

697 Vries, W.D., Reinds, G.J. Vel E., Intensive monitoring of forest ecosystems in Europe.
698 2-Atmospheric deposition and its impacts on soil solution chemistry. *For. Ecol.*
699 *Manage.* 174, 97-115, 2003.

700 Wang, T.J., Jin, L.S., Li, Z.K., Lam K.S., A modeling study on acid rain and
701 recommended emission control strategies in China. *Atmos. Environ.* 34, 4467-
702 4477, 2000.

703 West, A.J., Galy, A., Bickle, M., Tectonic and climatic controls on silicate weathering.
704 *Earth Planet. Sci. Lett.* 235, 211-228, 2005.

705 Wu, W., Zheng, H., Yang, J., Luo, C., Zhou, B., Chemical weathering, atmospheric CO₂
706 consumption, and the controlling factors in a subtropical metamorphic-hosted
707 watershed. *Chem. Geol.* 356, 141-150, 2013.

708 Xiang, L., Study on Coupling between Water and Carbon of Artificial Forests
709 Communities in Subtropical Southern China. Master Dissertation, Institute of
710 Geographical Sciences and Natural Sources, Chinese Academy of Sciences,
711 China (in Chinese), 2006.

712 Xu, H., Bi, X-H., Feng, Y-C., Lin, F-M., Jiao, L., Hong, S-M., Liu, W-G., Zhang, X.-
713 Y., Chemical composition of precipitation and its sources in Hangzhou, China.
714 *Environ. Monit. Assess.* 183:581-592, 2011.

715 Xu, Y., Wang C.Y., Zhao T., Using detrital zircons from river sands to constrain major

716 tectono-thermal events of the Cathaysia Block, SE China. *J. Asian Earth Sci.* 124,
717 1-13, 2016.

718 Xu, Z., Liu, C.-Q., Chemical weathering in the upper reaches of Xijiang River draining
719 the Yunnan-Guizhou Plateau, Southwest China. *Chem. Geol.* 239, 83-95, 2007.

720 Xu, Z., Liu, C.-Q., Water geochemistry of the Xijiang basin rivers, South China:
721 Chemical weathering and CO₂ consumption. *Appl. Geochem.* 25, 1603-1614,
722 2010.

723 Yoshimura, K., Nakao, S., Noto, M., Inokura, Y., Urata, K., Chen, M., Lin, P.W.,
724 Geochemical and stable isotope studies on natural water in the Taroko Gorge karst
725 area, Taiwan - chemical weathering of carbonate rocks by deep source CO₂ and
726 sulfuric acid. *Chem. Geol.* 177, 415-430, 2001.

727 Zhang, M., Wang, S., Wu, F., Yuan, X., Zhang, Y., Chemical compositions of wet
728 precipitation and anthropogenic influences at a developing urban site in
729 southeastern China. *Atmos. Res.* 84, 311-322, 2007a.

730 Zhang, S.R., Lu, X. X., Higgitt, D. L., Chen, C.T.A., Sun, H.-G., Han, J.T., Water
731 chemistry of the Zhujiang (Pearl River): Natural processes and anthropogenic
732 influences. *J. Geophys. Res.* 112, F01011, 2007b.

733 Zhao, W., An analysis on the changing trend of acid rain and its causes in Fujian
734 Province. *Fujian Geogr.* 19, 1-5 (in Chinese), 2004.

735 Zhou, X.M., Li, W.X., Origin of Late Mesozoic igneous rocks in Southeastern China:
736 Implications for lithosphere subduction and underplating of mafic magmas.
737 *Tectonophysics* 326(3-4), 269-287, 2000.

738 Zhou, X.M., Sun, T., Shen, W.Z., et al., Petrogenesis of Mesozoic granitoids and
739 volcanic rocks in South China: A response to tectonic evolution. *Episodes* 29(1),
740 26-33, 2006.

741 ZJBGMR: Zhejiang Bureau of Geology and Mineral Resources, Regional Geology of
742 Zhejiang Province. Geol. Publ. House, Beijing, p. 617 (in Chinese with English
743 abstract), 1989.

Table 1 Chemical and carbon isotopic compositions of river waters in the Southeast Coastal Rivers Basin (SECRB) of China.

Rivers	Sample number	Date (M/D/Y)	pH	T °C	EC $\mu\text{s cm}^{-1}$	Na ⁺ μM	K ⁺ μM	Mg ²⁺ μM	Ca ²⁺ μM	F ⁻ μM	Cl ⁻ μM	NO ₃ ⁻ μM	SO ₄ ²⁻ μM	HCO ₃ ⁻ μM	SiO ₂ μM	TZ ⁺ μEq	TZ ⁻ μEq	NICB %	$\delta^{13}\text{C}$ ‰	TDS mg l^{-1}
Qiantang*	1	07-8-10	7.42	28.78	190	347	197	106	473	12.0	303	62.6	147	1130	148	1703	1789	-5.0	-19.0	144
	2	07-9-10	7.60	23.84	146	87.5	204	80.9	496	11.7	75.2	124	121	907	156	1446	1348	6.7	-19.8	119
	3	07-9-10	7.37	27.83	308	555	233	208	698	41.8	312	223	437	1170	170	2601	2579	0.9	-17.8	204
	4	07-10-10	7.27	26.28	177	176	135	116	544	15.7	151	142	170	985	175	1632	1618	0.8	-19.3	135
	5	07-10-10	7.05	24.15	123	130	101	66.2	349	17.7	94.3	124	157	529	169	1061	1061	0.0	-18.7	91.2
	6	07-10-10	7.24	23.75	140	97.6	69.7	81.0	451	20.0	62.1	109	204	703	164	1231	1282	-4.2	-21.3	106.6
	7	07-11-10	7.40	23.23	107	92.5	70.5	68.3	327	14.9	74.9	104	147	486	156	954	960	-0.6	-21.0	82.2
	8	07-11-10	7.16	27.61	281	361	87.5	128	469	26.8	245	191	239	810	179	1642	1724	-5.0	-12.9	137.5
	9	07-11-10	7.02	26.48	140	275	120	60.7	319	36.2	199	150	180	437	236	1155	1146	0.8	-13.9	100.2
	10	07-12-10	7.05	24.24	99	205	114	58.3	285	14.6	191	114	132	305	278	1005	874	13.1	-20.9	85.4
	11	07-12-10	7.05	27.01	102	123	133	49.8	284	18.6	86.5	123	144	377	183	924	874	5.4	-19.2	79.4
	12	07-12-10	7.99	24.18	260	50.0	85.4	212	993	-	66.8	153	235	1822	172	2546	2512	1.4	-17.6	205.2
	13	07-12-10	7.86	24.59	231	43.5	88.4	189	859	-	55.1	97.6	169	1763	170	2228	2253	-1.1	-18.7	185.4
	14	07-12-10	7.69	22.66	131	44.1	81.0	113	458	-	19.1	95.2	107	920	143	1266	1248	1.4	-18.1	106.8
	15	07-12-10	7.65	24.48	106	61.1	98.3	87.9	335	-	37.2	68.3	112	663	164	1005	992	1.4	-18.6	87.3
	16	07-12-10	7.46	23.68	125	64.3	108	117	406	-	25.9	75.0	174	687	164	1218	1136	6.7	-20.0	98.8
	17	07-13-10	7.33	24.08	139	59.8	116	136	429	-	29.6	80.4	209	752	162	1305	1281	1.9	-20.8	108.1
	18	07-10-10	7.27	25.74	141	163	114	69.6	396	27.3	126	148	161	597	153	1209	1195	1.1	-21.0	101.0
Cao'e	19	07-16-10	7.17	22.27	108	212	86.3	69.4	183	5.1	151	148	114	384	216	803	912	-13.5	-21.2	79.1
	20	07-16-10	7.06	26.57	182	401	77.6	145	275	18.3	269	185	245	534	215	1318	1478	-12.2	-20.5	116.9
	21	07-16-10	7.14	27.26	171	333	91.3	164	362	18.1	224	194	207	658	225	1475	1490	-1.0	-20.9	123.3
	22	07-16-10	7.08	27.17	173	346	94.4	168	364	18.8	247	200	211	656	222	1506	1526	-1.3	-13.0	125.2
Ling	23	07-15-10	7.07	24.14	52	164	42.9	34.9	140	4.9	40.7	61.5	68.3	277	190	558	516	7.6	-12.8	52.1
	24	07-15-10	7.02	26.04	74	169	92.0	34.2	150	6.4	87.0	77.3	92.8	272	196	629	622	1.1	-20.8	59.5
	25	07-16-10	7.34	25.03	92	159	80.1	47.3	235	19.3	78.0	71.4	105	455	187	804	815	-1.4	-22.5	73.9
	26	07-16-10	7.40	26.75	113	216	77.8	57.1	249	20.2	133	90.0	115	494	196	905	946	-4.5	-12.7	82.8
	27	07-16-10	7.39	26	89	174	86.4	56.4	209	9.0	99.3	78.4	99.9	420	199	792	798	-0.8	-14.0	72.7
	28	07-15-10	6.79	22.33	75	159	82.7	44.1	143	-	107	61.8	83.4	306	144	616	641	-4.1	-21.1	56.5
	29	07-15-10	8.24	27.15	129	228	92.1	83.1	317	17.2	177	90.5	120	641	194	1120	1148	-2.5	-19.2	97.8
Ou	30	07-13-10	8.08	28.45	48	95.2	107	38.4	92.1	15.2	31.8	43.3	47.4	291	221	463	461	0.4	-21.7	50.6
	31	07-13-10	6.71	22.97	32	60.7	106	12.6	65.0	10.8	28.9	45.0	48.9	158	169	322	329	-2.2	-23.8	36.9
	32	07-13-10	7.18	27.59	73	107	127	36.2	175	4.3	57.1	111	92.0	283	210	655	634	3.2	-23.4	62.9
	33	07-13-10	6.94	24.2	44	76.9	112	20.0	99.1	10.9	27.9	63.1	58.6	249	184	427	457	-7.0	-22.5	47.5
	34	07-14-10	7.16	27.45	90	187	127	41.2	199.5	17.0	85.6	102	116	367	251	796	787	1.1	-22.4	76.5
	35	07-14-10	6.97	24.56	54	105	50.9	29.2	122	12.2	46.1	67.8	73.1	218	193	460	478	-4.1	-22.5	47.9
	36	07-14-10	6.82	21.12	31	76.4	133	12.7	74.5	7.7	20.7	36.8	49.1	192	162	383	348	9.3	-	39.5
	37	07-14-10	6.82	23.69	45	89.5	105	19.0	97.8	10.6	39.6	52.8	59.1	231	185	428	441	-3.0	-22.9	46.2
	38	07-15-10	6.92	24.69	37	100	89.3	21.1	49.7	1.7	36.9	45.5	52.7	153	202	331	341	-2.9	-	38.9
	39	07-15-10	6.90	23.86	35	92.2	92.0	19.8	61.4	1.9	43.9	47.9	55.5	139	193	347	342	1.4	-22.3	38.5
	40	07-15-10	7.09	25.56	47	117	112	25.7	83.4	8.0	52.4	63.1	57.4	232	193	447	462	-3.3	-22.5	48.1
	41	07-14-10	6.97	24.25	53	102	107	27.6	119	13.4	43.5	59.4	73.2	277	183	502	526	-4.9	-13.7	52.3

Feiyun	42	07-17-10	7.28	25.19	38	94.0	81.7	24.0	75.6	11.4	59.9	45.7	51.9	149	151	375	358	4.5	-	37.2
	43	07-17-10	7.08	25.61	46	101	79.9	33.9	93.4	4.6	66.2	55.1	52.8	223	151	435	450	-3.3	-23.7	43.5
Jiaoxi	44	07-17-10	7.52	26.92	47	116	81.5	25.2	92.0	4.1	73.3	80.3	25.0	226	151	432	430	0.5	-23.4	43.0
	45	07-17-10	7.45	27.46	61	152	90.2	34.2	119	-	136	59.8	53.5	238	184	548	542	1.2	-23.1	51.8
Huotong	46	07-18-10	6.90	27.66	53	127	88.1	33.4	94.4	7.0	123	93.1	30.4	209	177	471	486	-3.3	-14.4	47.4
	47	07-18-10	7.34	24	43	116	78.8	26.1	58.4	5.4	68.7	49.7	20.1	197	190	364	355	2.3	-22.8	39.6
Ao	48	07-19-10	7.24	31.44	124	294	121	102	209	24.3	204	73.6	52.0	717	370	1036	1100	-6.1	-19.4	105.4
	49	07-19-10	7.13	27.82	46	109	96.3	30.0	73.8	-	72.0	51.3	22.5	234	236	413	402	2.6	-	46.2
Min	50	07-18-10	6.98	28.65	53	140	88.4	40.8	100	3.0	82.9	58.6	20.9	294	233	511	477	6.6	-22.3	52.2
	51	07-27-10	7.11	28.4	42	116	92.0	40.5	119	18.0	43.9	35.5	26.0	382	182	526	513	2.4	-19.4	52.7
	52	07-27-10	7.17	30	51	102	97.9	41.7	107	4.6	29.4	45.3	35.0	350	221	496	495	0.2	-	53.3
	53	07-27-10	7.08	29.4	99	214	92.7	46.4	126	18.4	50.1	39.8	118	327	154	651	654	-0.4	-20.8	74.0
	54	07-27-10	7.06	29.1	44	107	99.6	28.1	114	16.4	18.7	36.4	44.3	305	265	491	449	8.5	-17.6	53.6
	55	07-27-10	7.42	29.4	57	139	93.7	49.8	113	3.1	67.1	56.3	26.6	384	236	558	561	-0.5	-16.4	58.6
	56	07-27-10	7.12	27.8	51	103	91.0	50.8	106	4.7	82.8	35.1	63.5	249	225	507	494	2.5	-	51.3
	57	07-27-10	7.08	27.5	40	125	45.0	36.8	107	12.1	43.6	44.5	29.3	288	211	457	435	5.0	-21.1	47.4
	58	07-27-10	6.99	27.2	52	121	98.0	42.4	115	16.7	87.1	36.6	70.9	277	228	535	542	-1.4	-11.4	55.3
	59	07-27-10	6.87	29	59	154	91.4	59.4	124	16.5	77.8	36.7	88.3	272	222	612	563	8.0	-20.3	57.2
	60	07-27-10	7.31	27.1	78	109	92.1	59.1	181	21.2	123	37.5	78.4	355	202	682	672	1.4	-18.7	63.1
	61	07-27-10	7.22	27.8	37	122	83.3	52.8	142	17.4	111	37.3	80.4	288	221	596	597	-0.2	-22.3	58.1
	62	07-27-10	7.16	28.1	58	104	83.3	59.3	163	24.0	34.6	34.5	118	294	214	632	599	5.2	-13.4	59.5
	63	07-27-10	7.26	28.3	87	139	86.1	60.9	191	14.8	48.0	93.0	109	347	226	729	707	3.0	-21.4	68.6
	64	07-27-10	7.00	28.8	87	127	93.1	58.7	195	6.6	59.8	81.1	60.9	480	232	729	743	-2.0	-11.0	74.0
	65	07-28-10	6.97	27.9	37	163	82.1	52.2	140	20.2	53.1	60.0	106	306	221	630	632	-0.2	-	61.9
	66	07-13-10	7.07	27.96	59	91.9	110	40.0	127	24.8	62.0	79.3	62.3	249	228	535	515	3.8	-	54.8
	67	07-28-10	7.12	29.7	38	108	93.4	45.9	133	12.4	48.3	34.0	56.6	368	220	560	564	-0.7	-	57.7
	68	07-27-10	7.03	29.9	62	128	96.7	57.6	148	23.3	81.6	36.8	74.1	374	203	635	641	-0.9	-12.4	61.7
	69	07-27-10	7.01	28.8	60	102	89.1	73.6	138	9.6	50.6	74.1	32.7	417	233	615	607	1.3	-21.0	62.3
	70	07-27-10	7.06	26.5	37	93.5	93.1	34.7	87.3	-	26.6	34.8	37.1	312	222	431	448	-3.9	-13.1	49.1
	71	07-27-10	7.09	26.5	25	62.6	92.7	27.0	61.5	4.7	21.5	18.6	43.4	191	154	332	318	4.2	-16.0	35.3
	72	07-28-10	7.07	30.1	39	76.3	87.9	35.1	87.6	7.4	43.1	36.6	35.5	266	175	409	416	-1.7	-19.4	43.5
	73	07-27-10	7.01	28.7	47	84.9	95.4	56.7	106	12.7	51.8	49.2	57.2	315	211	506	531	-4.8	-	53.8
	74	07-27-10	6.85	28.7	50	93.6	85.9	52.4	107	14.1	62.8	57.5	57.0	252	217	498	487	2.2	-19.9	50.9
	75	07-27-10	7.11	29.7	69	117	85.2	73.4	159	7.6	63.7	75.2	47.4	418	230	666	652	2.2	-22.2	65.0
	76	07-28-10	6.93	28.9	59	112	88.0	61.8	122	6.0	57.4	89.3	42.0	349	224	568	580	-2.2	-22.0	58.8
	77	07-21-10	7.76	32.4	51.2	163	85.5	52.8	151	20.2	55.3	70.3	78.6	372	175	656	655	0.3	-12.5	61.8
	78	07-28-10	7.29	26.8	106	129	75.3	84.0	321	24.0	56.2	41.0	166	599	202	1013	1028	-1.4	-16.3	90.3
79	07-21-10	7.09	26.96	56	112	87.6	37.1	129	4.5	51.5	44.9	61.9	327	276	531	547	-2.9	-22.2	59.1	
80	07-21-10	7.64	33.37	83	114	96.2	60.6	151	16.7	53.0	40.6	102	371	242	633	670	-5.8	-12.8	66.2	
81	07-21-10	7.83	31.27	65	131	102	52.7	141	16.1	45.3	49.7	91.8	324	239	620	603	2.8	-13.4	61.8	
82	07-21-10	6.84	28.35	66	132	101	52.5	141	5.8	63.8	54.1	91.6	304	243	621	606	2.5	-22.7	61.5	
83	07-21-10	7.42	30.7	98	217	113	59.2	210	18.4	98.7	63.5	84.7	496	320	868	827	4.6	-18.9	84.5	
84	07-27-10	7.26	26.3	46	104	102	29.7	121	3.6	55.2	51.9	55.5	294	193	507	512	-0.9	-21.6	51.9	
85	07-27-10	7.07	25.4	30	73.3	99.2	19.6	78.8	-	22.9	40.0	49.2	203	170	369	365	1.3	-21.1	39.8	
86	07-27-10	7.50	27.3	45	102	102	26.5	114	2.4	35.1	39.7	57.2	260	217	484	449	7.3	-15.7	49.6	
87	07-27-10	7.47	26.9	51	141	100	43.6	109	7.9	79.7	42.4	57.7	311	217	547	548	-0.3	-20.1	55.6	

	88	07-19-10	7.99	31.74	63	167	96.5	33.5	115	8.0	105	35.5	38.1	331	218	561	548	2.3	-13.5	55.9
	89	07-21-10	6.77	28.19	65	132	93.6	56.0	145	15.6	60.6	78.8	75.4	333	243	627	624	0.5	-22.6	63.3
Jin	90	07-27-10	7.36	25.8	128	126	94.8	88.9	406	22.9	51.4	39.4	229	595	208	1211	1143	5.6	-20.7	100
	91	07-27-10	7.40	26.9	123	143	103	82.7	347	21.0	83.5	203	182	463	226	1105	1115	-0.9	-21.3	98.4
	92	07-27-10	7.00	27.4	88	170	98.8	56.8	205	7.2	137	117	106	327	205	793	792	0.1	-22.5	71.8
	93	07-27-10	7.32	28.7	73	201	116	87.1	318	20.0	93.5	41.5	189	508	267	1128	1020	9.6	-21.7	95.3
Jiulong	94	07-30-10	6.50	23.47	29	72.3	92.4	22.8	59.8	12.4	25.1	27.0	50.0	189	213	330	341	-3.4	-18.1	40.1
	95	07-30-10	7.06	29.35	120	136	96.9	106	339	5.1	67.7	66.3	249	469	202	1124	1100	2.1	-20.8	94.2
	96	07-30-10	7.45	27.6	104	79.5	97.5	106	363	14.4	70.7	50.0	99.9	729	184	1116	1049	6.0	-18.9	93.7
	97	07-31-10	7.36	26.59	139	140	100	142	432	15.5	79.6	78.3	274	573	196	1388	1278	8.0	-19.7	108.8
	98	07-31-10	7.72	26.18	88	77.6	96.2	69.0	313	19.9	39.7	34.6	63.8	731	251	938	933	0.5	-18.4	89.4
	99	07-30-10	7.43	26.96	119	200	93.8	100.2	298	19.9	122	80.5	225	387	202	1091	1040	4.7	-20.5	89.5
	100	07-28-10	7.41	26.66	112	173	97.9	94.4	286	46.1	118	152	201	364	207	1033	1036	-0.3	-20.9	92.2
	101	07-29-10	7.16	29.35	82	151	110	55.4	178	4.9	71.2	170	53.2	385	305	727	732	-0.7	-21.2	76.1
	102	07-29-10	7.10	28.9	100	222	98.3	49.4	249	3.6	126	157	52.7	532	303	917	920	-0.3	-21.7	90.0
	103	07-28-10	7.20	31.15	138	339	111	81.2	277	9.2	280	285	88.6	515	317	1165	1256	-7.8	-19.0	112
	104	07-28-10	7.16	27.09	101	261	95.8	81.7	235	40.3	173	80.1	174	291	136	990	892	9.9	-24.3	75.4
Zhang	105	07-28-10	8.08	30.6	93	195	96.1	61.1	167	16.8	157	193	55.2	281	288	748	741	0.9	-21.5	73.8
Dongxi	106	07-28-10	7.20	30.9	78	263	99.0	41.5	115	14.5	238	65.3	30.0	283	309	675	646	4.4	-20.8	66.7
Huangang	107	07-28-10	7.40	30.5	99	253	85.6	53.0	154	7.7	190	63.5	56.4	460	278	754	827	-9.6	-20.0	77.4
Han	108	07-31-10	7.31	27.1	68	136	61.5	45.2	195	16.1	37.7	45.3	93.7	345	218	678	615	9.2	-21.9	62.0
	109	07-30-10	7.38	26.94	88	116	103	63.6	265	6.4	53.4	72.2	84.9	584	244	876	879	-0.4	-20.4	83.7
	110	07-30-10	6.66	25.55	71	114	96.2	47.6	168	8.0	56.9	54.6	143	230	203	642	628	2.2	-17.9	59.7
	111	07-30-10	6.66	27.76	83	135	104	63.8	203	8.6	54.5	74.9	173	302	336	774	777	-0.4	-20.6	78.7
	112	07-30-10	7.31	30.81	56	168	74.0	39.1	118	13.5	62.9	44.4	81.4	237	245	556	507	8.8	-21.4	54.6
	113	07-31-10	7.28	28.73	98	137	99.3	85.6	270	9.2	88.8	59.1	118	565	233	948	949	-0.1	-19.7	86.6
	114	07-31-10	7.27	31.42	123	193	105	98.2	319	20.7	120	102	157	570	229	1132	1107	2.2	-19.7	98.2
	115	07-30-10	7.43	29.89	85	115	97.5	65.5	244	6.5	46.5	58.6	103	511	251	832	822	1.1	-20.8	79.3
	116	07-31-10	7.61	30.98	99	123	104	85.9	264	5.6	58.8	90.9	108	588	98	926	952	-2.9	-20.0	79.4
	117	07-31-10	7.31	29.96	93	151	103	78.1	250	15.4	68.0	99.1	173	379	233	909	891	1.9	-21.9	81.8
	118	07-31-10	7.35	28.4	2	233	84.2	101	323	12.8	84.0	101	203	460	229	1165	1051	9.8	-21.1	94.7
	119	07-31-10	7.67	30.38	93	136	87.8	73.6	231	16.4	64.6	94.4	184	382	226	834	909	-9.1	-20.8	80.5
Rong	120	07-30-10	7.57	31.83	68	193	79.1	50.3	146	16.4	192	84.0	31.5	344	309	664	683	-2.8	-20.3	65.8
	121	07-30-10	6.96	30.62	94	509	103	56.1	213	15.9	511	78.5	82.3	379	222	1150	1133	1.5	-20.0	94.4

TZ⁺ is the total cationic charge; TZ⁻ is the total anionic charge; NICB is the normalized inorganic charge balance and TDS is the total dissolved solid. *data of major ion composition are from Liu et al. (2016).

Ding	Xikou	11.14	9.228	1207	17	6	46	32	0.31	0.18	9.0	33.3	19.1	52.4	341	196	249	212
Mei	Hengshan	10.29	12.95	794	12	13	31	44	0.21	0.32	5.7	16.6	24.5	41.1	212	252	173	157
Whole SECRB		207	167	1240					3.95	4.09	7.8	23.7	24.5	48.1	287	251	218	191

^a Cat_{sil} are calculated based on the sum of cations from silicate weathering.

^b SWR, CWR and TWR represent silicate weathering rates (assuming all dissolved silica is derived from silicate weathering), carbonate weathering rates and total weathering rates, respectively.

^c CO₂ consumption rate with assumption that all the protons involved in the weathering reaction are provided by carbonic acid.

^d Estimated CO₂ consumption rate by silicate weathering when H₂SO₄ from acid precipitation is taken into account.

^e Estimated CO₂ consumption rate by silicate weathering when H₂SO₄ and HNO₃ from acid precipitation is taken into account.

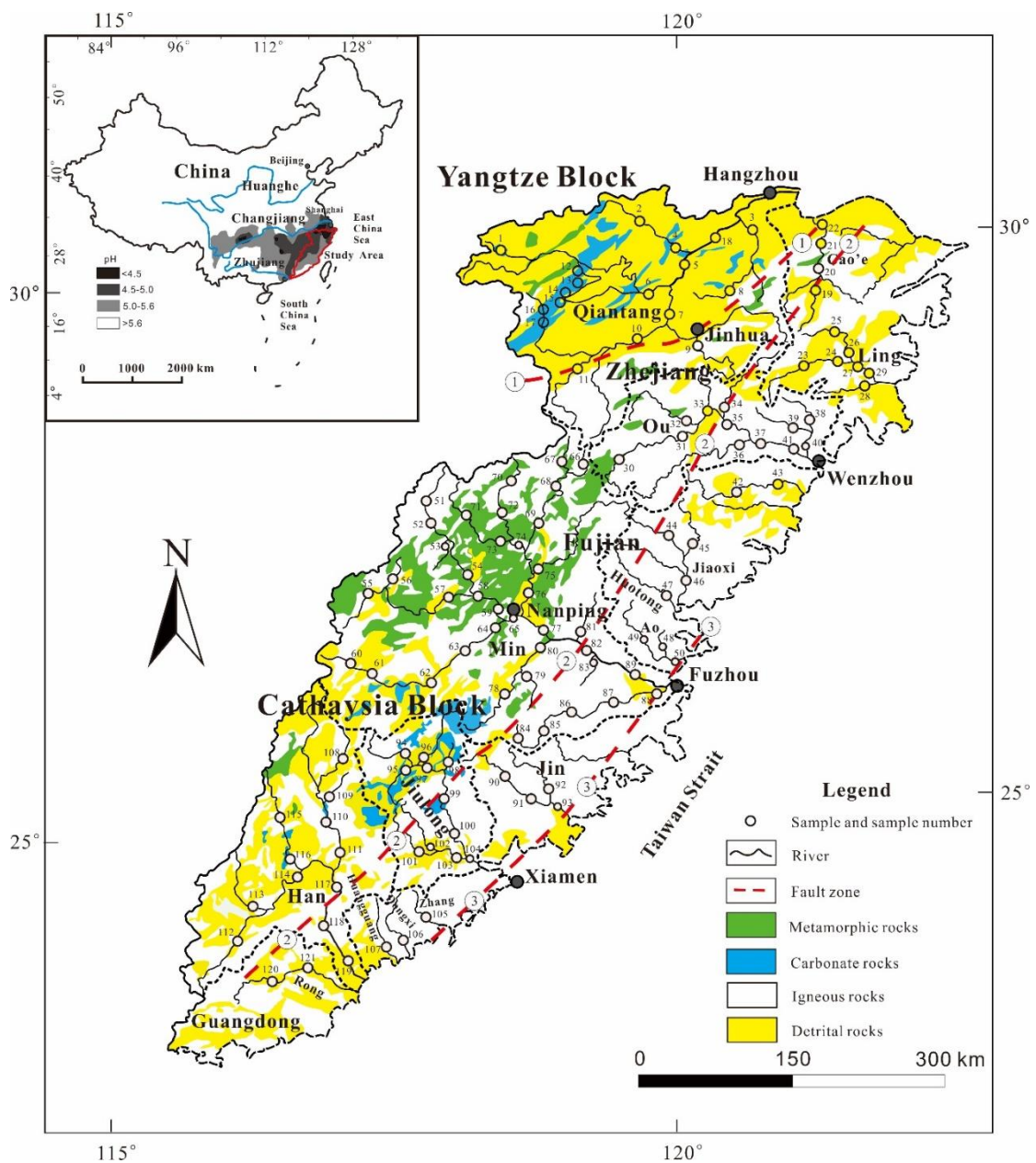


Fig. 1. Sketch map showing the lithology, sampling locations, and sample number of the SECRs drainage basin, and regional rain water pH ranges are shown in the sketch map at the upper-left. (modified from Zhou and Li, 2000; Shu et al., 2009; Xu et al., 2016, rain water acidity distribution of China mainland is from State Environmental Protection Administration of China). ① Shaoxing-Jiangshan fault zone; ② Zhenghe-Dapu fault zone; ③ Changle-Nanao fault zone. The figure was created by CorelDraw software version 17.1.

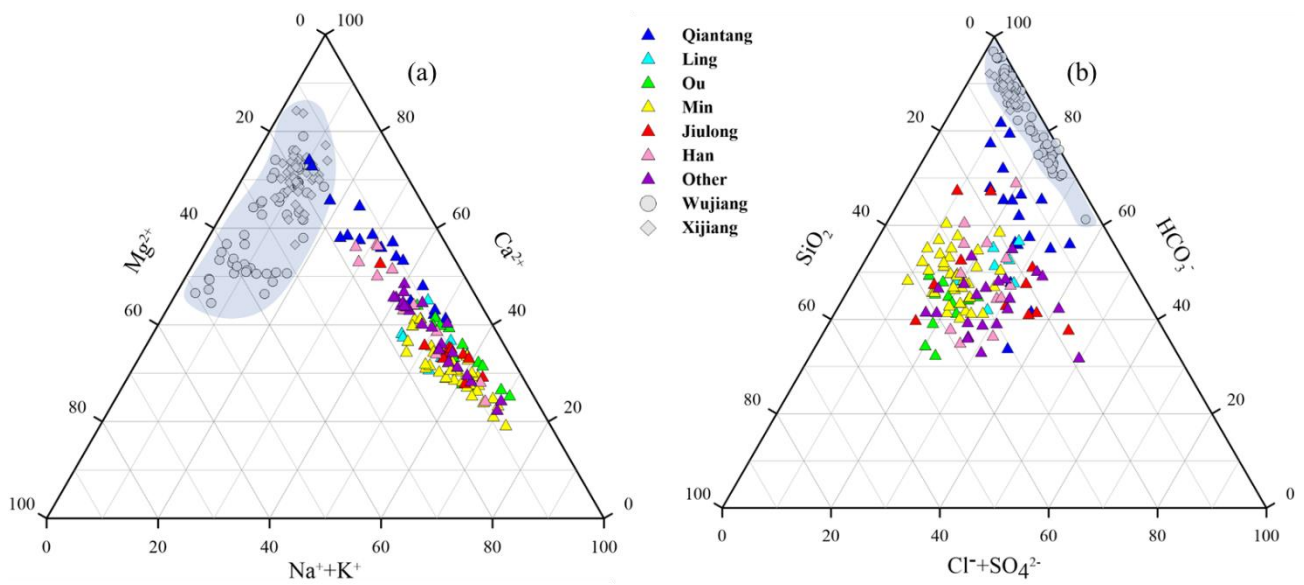


Fig. 2. Ternary diagrams showing cations (a), anions and dissolved SiO_2 (b) compositions of river waters in the SECRB. Chemical compositions from case studies of rivers draining carbonate rocks (the Wujiang and the Xijiang) are also shown for comparison (data from Han and Liu 2004; Xu and Liu 2007, 2010)

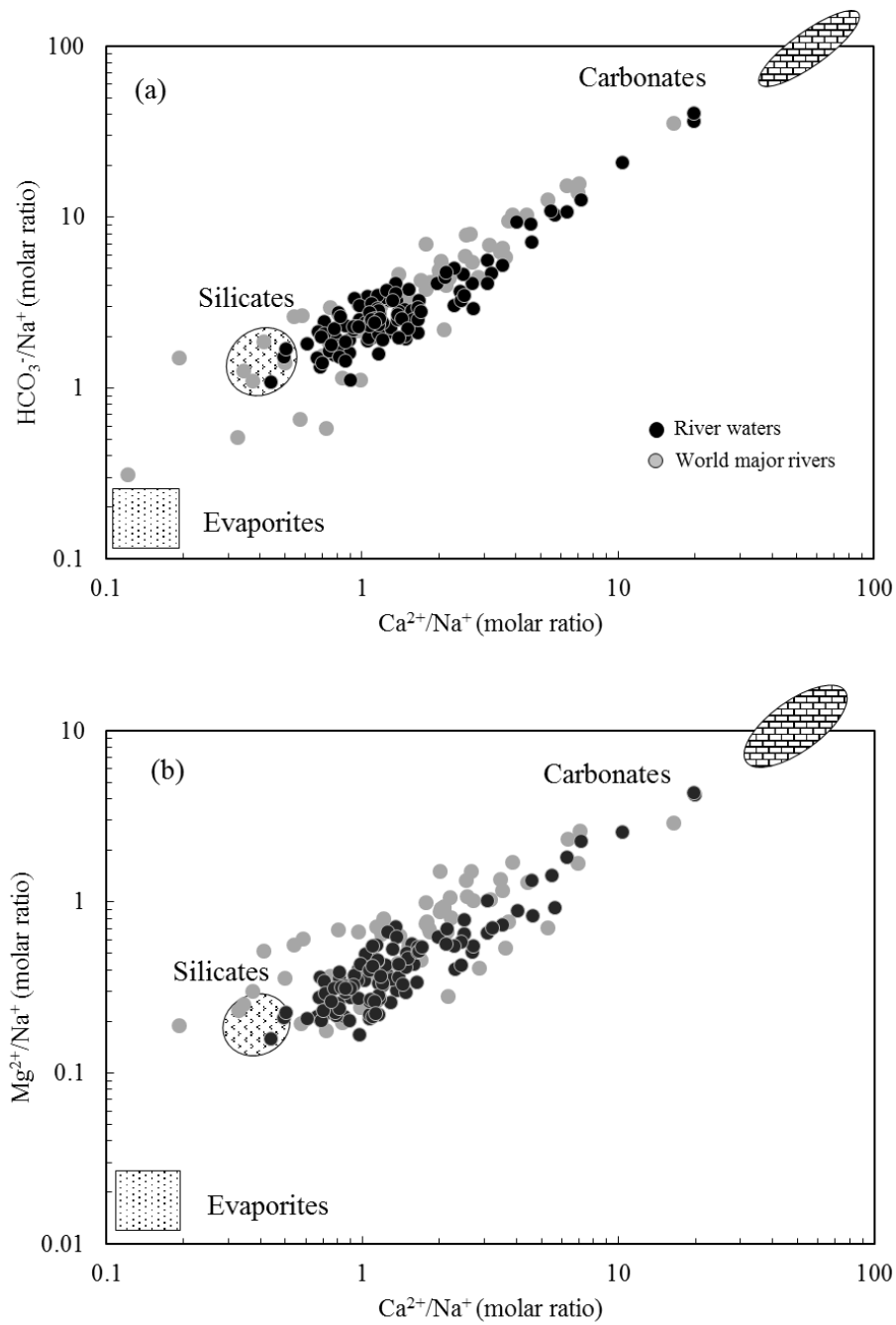


Fig. 3. Mixing diagrams using Na-normalized molar ratios: $\text{HCO}_3^-/\text{Na}^+$ vs. $\text{Ca}^{2+}/\text{Na}^+$ (a) and $\text{Mg}^{2+}/\text{Na}^+$ vs. $\text{Ca}^{2+}/\text{Na}^+$ (b) for the SECRB. The samples mainly cluster on a mixing line between silicate and carbonate end-members. Data for world major rivers are also plotted (data from Gaillardet et al. 1999).

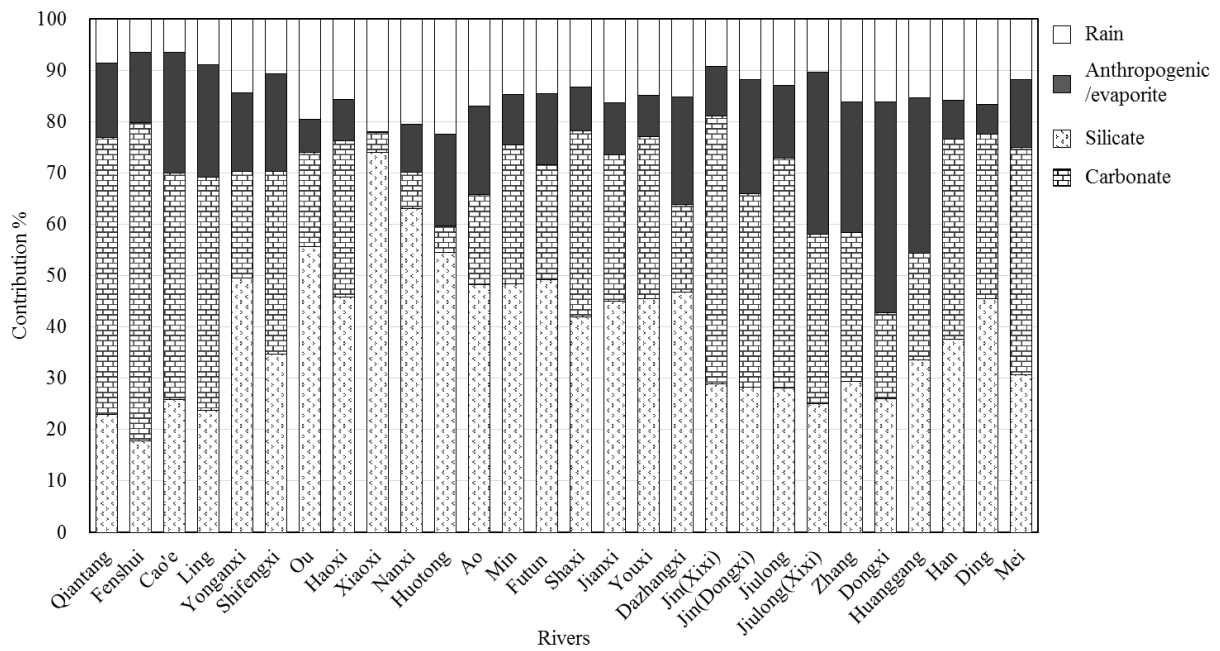


Fig. 4. Calculated contributions (in %) from the different reservoirs to the total cationic load for major rivers and their main tributaries in the SECRB. The cationic loads are the sum of Na^+ , K^+ , Ca^{2+} and Mg^{2+} from different reservoirs.

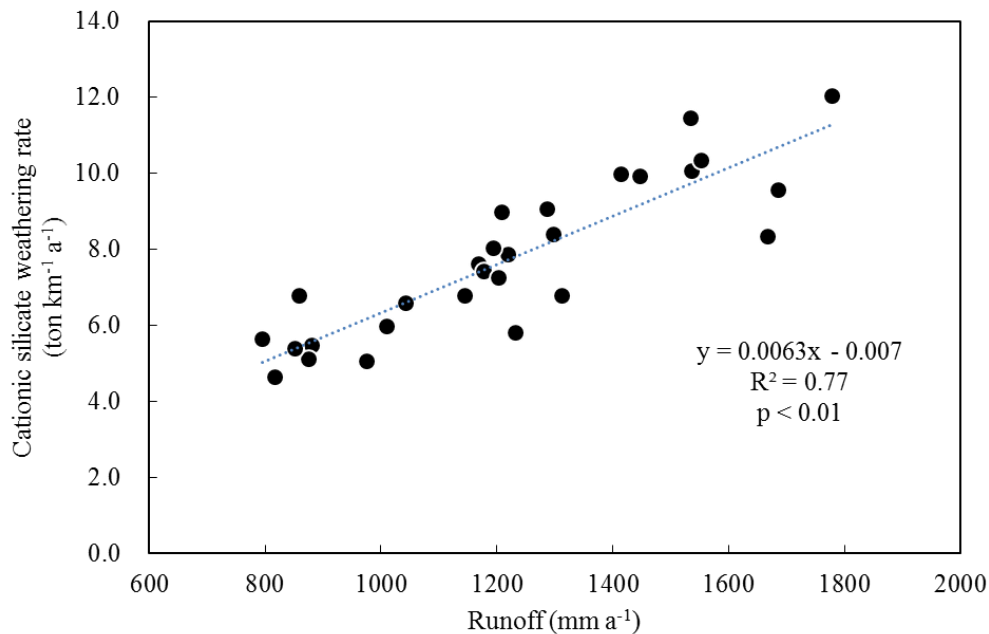


Fig. 5. Plots of the cationic-silicate weathering rate (Cat_{sil}) vs. runoff for the SECRB

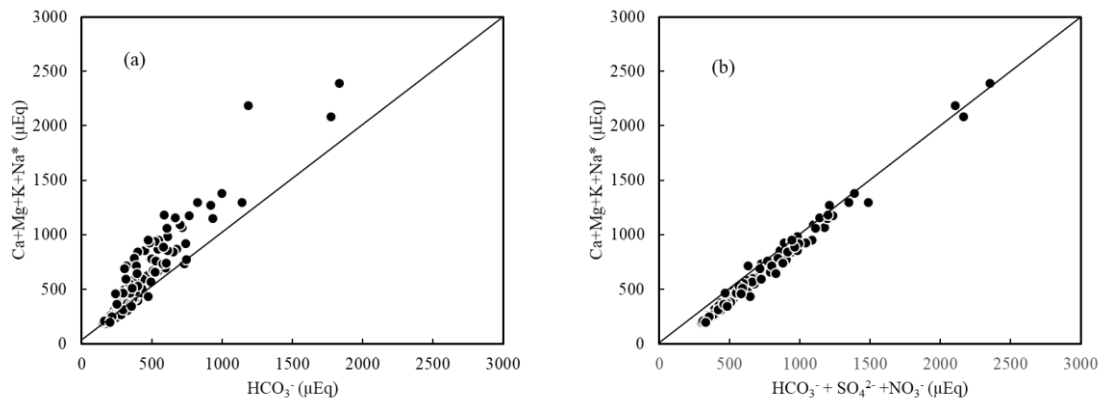


Fig. 6. Plots of total cations derived from carbonate and silicate weathering vs. HCO_3^- (a) and $\text{HCO}_3^- + \text{SO}_4^{2-} + \text{NO}_3^-$ (b) for river waters in the SECRB.

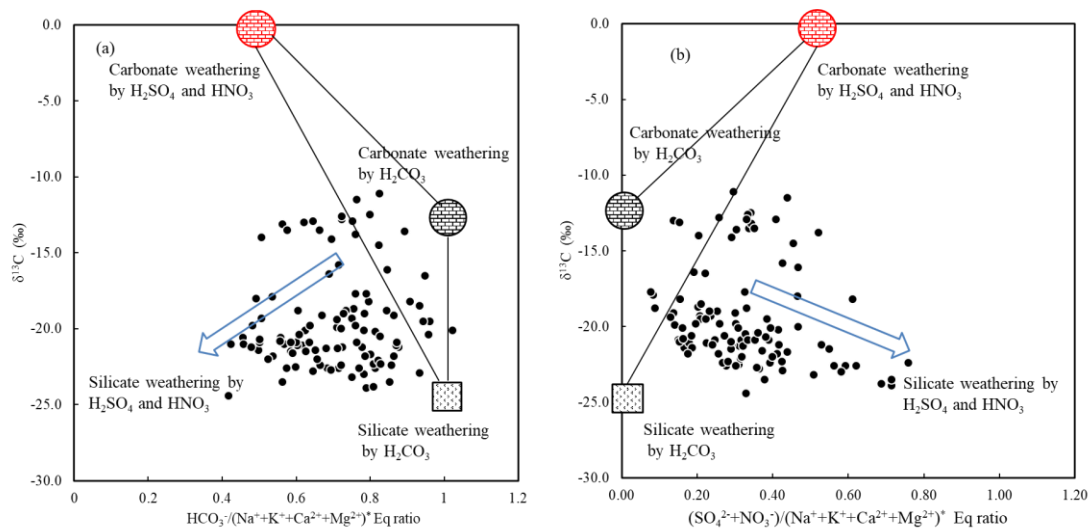


Fig. 7. $\delta^{13}\text{C}_{\text{DIC}}$ vs. $\text{HCO}_3^- / (\text{Na}^+ + \text{K}^+ + \text{Ca}^{2+} + \text{Mg}^{2+})^*$ (a) and $(\text{SO}_4^{2-} + \text{NO}_3^-) / (\text{Na}^+ + \text{K}^+ + \text{Ca}^{2+} + \text{Mg}^{2+})^*$ equivalent ratio (b) in river waters draining the SECRB (* noted concentrations corrected for atmospheric and anthropogenic inputs). The plots show that most waters deviate from the three end-member mixing area (carbonate weathering by carbonic acid and sulfuric acid and silicate weathering by carbonic acid), illustrating the effects of sulfuric and nitric acid on silicate weathering.